Building and Environment 219 (2022) 109224

Contents lists available at ScienceDirect

Building and Environment

journal homepage: www.elsevier.com/locate/buildenv

The emission and dynamics of droplets from human expiratory activities and COVID-19 transmission in public transport system: A review

Qiaoqiao Wang [a,b], Jianwei Gu [c,d,*], Taicheng An [c,d]

[a] Institute for Environmental and Climate Research, Jinan University, 511443, Guangzhou, China
[b] Guangdong-Hong Kong-Macau Joint Laboratory of Collaborative Innovation for Environmental Quality, 511443, Guangzhou, China
[c] Guangdong-Hong Kong-Macao Joint Laboratory for Contaminants Exposure and Health, Guangdong Key Laboratory of Environmental Catalysis and Health Risk Control, Institute of Environmental Health and Pollution Control, Guangdong University of Technology, 510006, Guangzhou, China
[d] Guangzhou Key Laboratory of Environmental Catalysis and Pollution Control, Guangdong Technology Research Center for Photocatalytic Technology Integration and Equipment Engineering, School of Environmental Science and Engineering, Guangdong University of Technology, 510006, Guangzhou, China

ARTICLE INFO

Keywords:
Respiratory droplet
Transmission
Dynamic
Public transport
SARS-CoV-2
COVID-19

ABSTRACT

The public transport system, containing a large number of passengers in enclosed and confined spaces, provides suitable conditions for the spread of respiratory diseases. Understanding how diseases are transmitted in public transport environment is of vital importance to public health. However, this is a highly multidisciplinary matter and the related physical processes including the emissions of respiratory droplets, the droplet dynamics and transport pathways, and subsequently, the infection risk in public transport, are poorly understood. To better grasp the complex processes involved, a synthesis of current knowledge is required. Therefore, we conducted a review on the behaviors of respiratory droplets in public transport system, covering a wide scope from the emission profiles of expiratory droplets, the droplet dynamics and transport, to the transmission of COVID-19 in public transport. The literature was searched using related keywords in Web of Science and PubMed and screened for suitability. The droplet size is a key parameter in determining the deposition and evaporation, which together with the exhaled air velocity largely determines the horizontal travel distance. The potential transmission route and transmission rate in public transport as well as the factors influencing the virus-laden droplet behaviors and virus viability (such as ventilation system, wearing personal protective equipment, air temperature and relative humidity) were also discussed. The review also suggests that future studies should address the uncertainties in droplet emission profiles associated with the measurement techniques, and preferably build a database based on a unified testing protocol. Further investigations based on field measurements and modeling studies into the influence of different ventilation systems on the transmission rate in public transport are also needed, which would provide scientific basis for controlling the transmission of diseases.

1. Introduction

The Coronavirus disease 2019 (COVID-19) was first detected in 2019, and was soon declared as a global pandemic by the World Health Organization (WHO) on March 11, 2020. By April 30, 2022, 510 million confirmed cases and 6.2 million deaths were reported by WHO [1]. The unexpected rapid spread of COVID-19 worldwide was largely associated with the convenient and advanced national and international public transport system, including flights, trains, buses, etc. [2,3]. For example, 4.3 billion journeys were conducted through the global aviation network in 2018 (11.8 million per day on average) [4], which could bring the virus to uninfected areas in a short time, even before the transmission of the epidemic was noticed. A recent study demonstrated that about 72% of the COVID-19 cases in New York in March 2020 had the same genome of severe acute respiratory syndrome coronavirus 2 (SARS-CoV-2) as those in Europe, indicating that transatlantic flights contributed largely to the early transmission in New York [5].

The public transport system is a special indoor environment with many passengers in an enclosed and confined space, favoring the propagation of diseases between passengers. There is ample evidence showing that the public transport environment contributes to the transmission of influenza and coronaviruses [6]. The transmission of

* Corresponding author. Guangdong-Hong Kong-Macao Joint Laboratory for Contaminants Exposure and Health, Guangdong Key Laboratory of Environmental Catalysis and Health Risk Control, Institute of Environmental Health and Pollution Control, Guangdong University of Technology, 510006, Guangzhou, China.
E-mail address: gujianwei@gdut.edu.cn (J. Gu).

https://doi.org/10.1016/j.buildenv.2022.109224
Received 3 November 2021; Received in revised form 3 May 2022; Accepted 20 May 2022
Available online 24 May 2022

SARS-CoV-2 in a variety of public transport systems has also been recently reported, including aircraft cabins [7,8], buses [9,10], trains [11,12] and cruise ships [13]. The ventilation system in public transport needs to provide conditioned air (heated or cooled) and to ensure passenger thermal comfort and an acceptable cabin air quality. Due to high population density, it requires high energy consumption. The ventilation systems and air distribution in common public transport systems such as buses, trains, airplanes are also different from the general indoor environment, and the main exposure and transmission routes of respiratory transmissible diseases are not fully understood yet.

Historically, public health communities have discovered two major transmission routes for respiratory-borne diseases, namely, short-distance droplet transmission and contact with contaminated surfaces (or fomites) [14,15]. At the early COVID-19 transmission stage, government and health agencies recommended social distancing to avoid the short-distance droplet transmission. Regarding the fomite route, hand washing and surface disinfection were recommended to reduce the possibility of picking up viruses via touching the contaminated surfaces. These measures are essential but may not be sufficient, as small droplets can evaporate quickly and remain in the air for a prolonged time. Aerosol scientists argued that viruses may also be transmitted via aerosols and be transported for a long distance. Therefore, adequate control measures against aerosol transmission must be considered additionally [16,17]. A case study in the bus by Cheng et al. [18] and Ou et al. [19] demonstrated that COVID-19 can be transmitted even if the infected person is far away (up to 9 m) from the index case (the first identified patient within a disease epidemic in a population), implying the possibility of exposure to virus-laden droplets via air or aerosol transmission route.

Nevertheless, airborne or droplet transmission is a complex process including droplet emission, evaporation, transport, deposition and the corresponding exposure of susceptible subjects. While the emission profiles and the consequent atmospheric behaviors of viruses-laden droplets vary with human respiratory activities (i.e. breathing, speaking, coughing, and sneezing) [20,21], different environmental and ventilation conditions in public transport also influence the transmission routes and the associated potential risk in the public transport systems [22–24]. Understanding these aspects is of vital importance for controlling COVID-19 and other transmissible respiratory tract diseases.

Here, we conducted a thorough review on both the emissions and the atmospheric behaviors of droplets or particles generated from expiratory activities, as well as the factors controlling the viral transmission in public transport systems with a focus on SARS-CoV-2. The review aimed to address the following questions: (1) What are the droplet/particle emission profiles from the human expiratory activities? (2) How do droplets transport, deposit, and evaporate? (3) What are the main factors controlling the behaviors of droplets or particles in the public transport systems?

2. Methods

In this review paper, literature was collected by searching in Web of Science and PubMed using keywords followed by manual screening for suitable topics and scopes. The keywords used in Web of Science included “emission”, “aerosol”, droplet”, “respiratory”, “coughing”, “sneezing”, “speaking”, “evaporation”, “dynamic”, “SARS-CoV-2”, “COVID-19”, “bus”, “subway”, “metro”, “underground”, “vehicle”, “train”, “rail”, “airplane”, “flight”, “public transport/transportation”, “face mask”, “filtration”, and “virus survival”. For COVID-19 transmission in public transport, literature search in PubMed was also conducted using keywords of “SARS-CoV-2”, “COVID-19”, “bus”, “subway”, “metro”, “underground”, “vehicle”, “train”, “rail”, “airplane”, and “flight”. Some of the papers were collected by cross-referencing other reviewed papers.

For the content in Sections 4.2.3 and 5 on the modeling and transmission of COVID-19 in public transport, a systematic review approach was used. Specifically, 2172 search results were obtained through searching in Web of Science and PubMed by December 16, 2021. After screening for duplication, scope and suitability, 47 papers were selected and included.

3. Droplet emission profiles from human expiratory activities

3.1. Number and size distribution

Three main methods have been applied to study the droplet number and size from expiratory activities: optical microscopy, on-line particle size spectrometer and on-site detection techniques. Optical microscopy, applied in early studies, uses collection media such as glass slides to collect deposited droplets, and then the stains of droplets are counted and measured with a microscope [20,25]. Dyes are commonly applied in the mouth to leave a colorful stain, while no dye is needed if water-sensitive paper is used. Although the microscope is capable of measuring stains as small as 0.25–0.50 μm, the method is only effective in measuring droplets >10 μm, because small droplets do not deposit effectively on the collection media but instead remain airborne for an extended time. Only a few studies endeavored to collect small droplets (<10 μm) by air sampling followed by microscope analysis (e.g. Duguid [20], Loudon and Roberts [25]).

The on-line particle size spectrometer uses an aerosol instrument with a tubing system to measure particles in a wide size range, focusing on small ones in general [26–28]. For instance, the Aerodynamic Particle Sizer (APS), Optical Particle Counter (OPC) and Wide-Range Particle Spectrometer (WPS) are capable of detecting particles with a size range of a few hundred nanometers to 10–20 μm, while the Scanning Mobility Particle Sizer (SMPS) is used for particles in a size range of several nanometers to sub-micrometer. It is worth noting that droplets may dry out in the tubing system, leading to their size reduction, while droplets near the upper size detection limit (e.g. 10–20 μm) may be lost due to gravitational settling and inertia in the tubing system. More recently, some studies utilized on-site detection techniques such as Interferometric Mie Imaging and laser particle size analyzer to determine droplet sizes (e.g. Chao et al. [29] and Han et al. [30]). These methods measure the droplets in the open air and the sensors are located close to the mouth opening. This approach is not subject to particle loss associated with the tubing system and can measure both small and large droplets (e.g. 0.1–1000 μm in the study of Han et al. [30] or 2–2000 μm in the study of Chao et al. [29]).

Table 1 and Table 2 summarize the characteristics of the droplets emitted from respiratory activities including breathing, speaking, singing, coughing, and sneezing from previous studies. For breathing, results are only available based on the on-line particle size spectrometer, limited to particles with diameters smaller than 10–20 μm. Only the study by Asadi et al. [26] reports E_n of 0–2 s^{-1} (0–11 L^{-1}), which is at the lower end of the range of E_n for speaking or singing. Most studies report droplet concentrations in the exhaled breath in the range from 14 to 1.7 $\times$ 10^4 L^{-1}. The wide range spanning three orders of magnitude can be largely attributed to individual differences, as some individuals are “super emitters" [31]. The variation can also be partly explained by the change in breathing maneuver, with higher concentrations for breathing to residual volume or with airway closure [32,33]. The droplet sizes from breathing were mainly below 1.0 μm, with peaks at 0.07 μm, 0.2–0.5 μm and 0.75–1.0 μm in different studies. It is also possible that peaks at larger size could be omitted due to the detection limit associated with the on-line particle size spectrometer.

For speaking or singing, emissions were measured when counting 1 to 100 in English, which was defined as one event in most studies. Reported droplet number emission rates (E_n) are in a wide range of 100–6720 $event^{-1}$ [20,21,26,29,34]. The size distribution of emitted droplets also varies largely, with the main peaks located at ~1 μm, 6 μm, 12 μm, 63 μm, and 100 μm in different studies. Three studies have identified a bimodal size distribution, showing both a major peak at <

Table 1
Number and size distribution of the droplets emitted from breathing, speaking and singing.

Activity	Reference	Droplet Number	Droplet Number Size Distribution	Methods (detectable size range)
Breathing	Edwards et al., 2004 [31]	high emitter: 660–3.2 × 10^3 L^{-1} (exhaled air) low emitter: 14–71 L^{-1} (exhaled air)	NA[a]	on-line particle size spectrometer (OPC, > 0.085 μm)
	Almstrand et al., 2010 [32]	breathing to residual volume: 8.5 × 10^3 (810–2.8 × 10^4) L^{-1} breathing to closing point: 2.5 × 10^3 (330–1.3 × 10^4) L^{-1} breathing to functional residual capacity: 1.3 × 10^3 (69–5.3 × 10^3) L^{-1} tidal breathing: 230 (18–1.0 × 10^3) L^{-1}	peak at 0.3–0.4 μm	on-line particle size spectrometer (OPC, 0.3–20 μm)
	Morawska et al., 2009 [35]	natural breathing in (nose) and out (mouth): 92 L^{-1} natural breathing with nose: 50 L^{-1}	*GMD* ≤ 0.8 μm[b]	on-line particle size spectrometer (APS, 0.7–20 μm)
	Asadi et al., 2019 [26][c]	0–2 s^{-1} (0–11 L^{-1})[d]	peak at 0.75–1.0 μm	on-line particle size spectrometer (APS, 0.5–20 μm)
	Holmgren et al., 2010 [33]	tidal breathing: 1.1 × 10^4 (600–8.3 × 10^4) L^{-1} (SMPS); 60 (20–230) L^{-1} (OPC); airway closure: 1.7 × 10^4 (3.9 × 10^3–6.9 × 10^4) L^{-1} (SMPS); 5.3 × 10^3 (1.0 × 10^3–1.2 × 10^4) L^{-1} (OPC)	tidal breathing: *GMD* = 0.07 μm, *GSD* = 2.0; airway closure: a broad peak at 0.2–0.5 μm	on-line particle size spectrometer (SMPS, 0.01–0.43 μm; OPC, 0.3–20 μm)
Speaking	Duguid 1946 [20]	252 $event^{-1}$[e]	peak at 12 μm	optical microscopy (>20 μm)
	Loudon and Roberts 1967 [25]	1764 (1171–2687) $event^{-1}$	peak at 100 μm	optical microscopy (>20 μm)
	Johnson et al., 2011 [28]	NA	main peak at 1.6 and 2.5 μm; sub-peak at 145 μm	optical microscopy (>20 μm) and on-line particle size spectrometer (APS, 0.7–20 μm)
	Xie et al., 2009 [21]	760 (100–2749) $event^{-1}$ (without dye) 2273 (809–3738) $event^{-1}$ (with dye)	peak at 63 μm	optical microscopy (>20 μm) and on-line particle size spectrometer (OPC, 0.3–20 μm)
	Asadi et al., 2019 [26][c]	1–50 s^{-1} (100–5000 $event^{-1}$)[f]	peak at 0.9–1.2 μm	on-line particle size spectrometer (APS, 0.5–20 μm)
	Chao et al., 2009 [29]	112–6720 $event^{-1}$	10 mm from mouth: main peak at 6 μm; sub-peak at 137 μm; 60 mm from mouth: peak at 6 μm	on-site detection techniques (Interferometric Mie imaging for size) (2–2000 μm)
Singing	Loudon and Roberts 1968 [34]	669 $event^{-1}$	main peak at 0–2.9 μm; sub-peak at 56–114 μm	optical microscopy (>20 μm)

[a] NA: not available.
[b] *GMD*: geometric mean diameter.
[c] In Asadi et al. [26], the speaking experiment was pronouncing/a/and reading book passages.
[d] Conversion of s^{-1} to L^{-1} assuming an average exhalation rate of 16 m^3 per day as adopted from EPA Exposure Handbooks (EPA 2011).
[e] One event is defined as counting (either speaking or singing) from 1 to 100 in English.
[f] Conversion of s^{-1} to $event^{-1}$ assuming that it takes 100 s for one speaking event.

10 μm and a sub-peak at > 50 μm [28,29,34]. The study by Asadi et al. [26] suggested that E_n is linearly correlated with the vocalization loudness but the corresponding number size distribution is independent of loudness.

For coughing, reported E_n values vary over five orders of magnitude (40–5.0 × 10^6 $cough^{-1}$) and the main peaks of related size distributions are located at < 0.1 μm, ~1 μm, ~5 μm, 12 μm, and ~75 μm in different studies. Studies that observed bimodal or trimodal size distribution generally found a major mode below 10 μm and sub-modes above 60 μm, similar to the results for speaking and singing. The highest E_n from the study of Lee et al. (2019) (more than two orders of magnitude higher than the other studies) can be partly explained by its relatively low size detection limit (0.01 μm) due to the application of SMPS. This also explains the discrepancy in the locations of the main peaks of the size distributions: < 0.1 μm in the study of Lee et al. (2019) vs. ≥ 1 μm in the other studies. However, the detection limit cannot explain all the observed variations. For example, the study reporting the lowest E_n (40 $cough^{-1}$ by Xie et al. [21]) has a detection limit of >0.3 μm, while the study reporting the second highest E_n (~10^4 $cough^{-1}$ by Lindsley et al., 2012) only targets particles of 0.35–10 μm in size. Many factors including the placement and the movement of lips, tongues and teeth as well as the amount of secretion during the cough may influence the droplet emissions. In addition, the health status of the test subjects may be another important factor as people with respiratory diseases tend to produce more violent coughs than healthy people [25].

Only two studies were found for the case of sneezing. Duguid [20] reported a droplet emission rate of 1 × 10^6 $sneeze^{-1}$ with a unimodal size distribution peaking at 6 μm. In contrast, Han et al. [30] identified both unimodal (with geometric mean diameter (*GMD*) = 360 μm) and bimodal (*GMD* = 72 and 386 μm) volume size distributions. Note that the mode of volume size distribution reported by Han et al. [30] tends to shift towards larger size compared with the number size distribution reported by other studies and thus cannot be compared directly with the others.

In summary, current available results have demonstrated considerably large variations in both droplet emission rates (differing by 2–5 orders of magnitude) and size distributions for each respiratory activity among studies and also within individual studies. This can be attributed to individual differences, loudness of voice, health condition, and measurement methods applied in the studies. Intensive activities such as coughing and sneezing tend to have higher E_n as well as larger variation. However, considering the duration, total emissions from breathing and speaking can be of more importance. In addition, most respiratory activities can produce droplets both smaller and larger than 10 μm in size, which will have different aerodynamic behaviors and subsequent exposure routes in the public transport. It is also worth noting that the major modes are all below 10 μm for the results with bimodal size distribution, emphasizing the relatively high possibility of the spreading of virus-laden droplets via the aerosol transmission route.

3.2. Expiratory air velocity

The initial air velocity (v_0) generally increases with the intensity of the expiratory activities, with the highest v_0 reported by Bourouiba [37] for sneezing (10–30 m s^{-1}), followed by coughing (9.0–15.3 m s^{-1}) [38–41], speaking (1.08–4.07 m s^{-1}) [29], and breathing (1.08–1.64 m s^{-1}) [42]. Some studies suggest that v_0 values from coughing and speaking are higher for males than females, while the study by Xu et al.

Table 2
Number and size distribution of the droplets emitted from coughing and sneezing.

Activity	Reference	Droplet Number	Droplet Number Size Distribution	Methods (detectable size range)
Coughing	Duguid 1946 [20]	5000 cough^{-1}	peak at 12 μm	optical microscopy (>20 μm)
	Loudon and Roberts 1967 [25]	466 (50–1642) cough^{-1}	main peak at 4 μm; sub-peak at 69 μm	optical microscopy (>20 μm)
	Johnson et al., 2011 [28]	NA[a]	main peak at 1.6 and 1.7 μm; sub-peak at 123 μm	optical microscopy (>20 μm) and on-line particle size spectrometer (APS, 0.7–20 μm)
	Xie et al., 2009 [21]	40 (14–67) cough^{-1}	peak at 63–88 μm	optical microscopy (>20 μm) and on-line particle size spectrometer (OPC, 0.3–20 μm)
	Lindsley et al., 2012 [27]	$7.5 \times 10^4 \pm 9.7 \times 10^4$ cough^{-1} (when ill); $5.2 \times 10^4 \pm 9.9 \times 10^4$ cough^{-1} (after recovery)	a broad peak at 0.35–1.7 μm	on-line particle size spectrometer (WPS, 0.35–10 μm)
	Lee et al., 2019 [36]	5.0×10^6 (7.7×10^5–1.9×10^7) cough^{-1} (when ill); 1.4×10^6 (3.6×10^5–4.2×10^6) cough^{-1} (after recovery)	peak at < 0.1 μm	on-line particle size spectrometer (SMPS, 0.01–0.42 μm; OPC, 0.3–10 μm)
	Chao et al., 2009 [29]	947–2085 cough^{-1}	main peak at 6 μm (10 and 60 mm from mouth) sub-peak at 175 μm (10 mm from mouth)	on-site detection techniques (Interferometric Mie imaging, 2–2000 μm)
Sneezing	Duguid 1946 [20]	1×10^6 sneeze^{-1}	peak at 6 μm	optical microscopy (>20 μm)
	Han et al., 2013 [30][b]	NA	unimodal volume size distribution: *GMD* = 360.1 μm, *GSD* = 1.5;[c] bimodal volume size distribution: *GMD* = 72 μm, *GSD* = 1.5; *GMD* = 386.2 μm, *GSD* = 1.8	on-site detection techniques (Laser Particle Size Analyzer, 0.1–1000 μm)

[a] NA: not available.
[b] The study reported volume size distribution instead of number size distribution.
[c] *GMD*: geometric mean diameter, *GSD*: geometric standard deviation.

[42] found slightly higher velocities from breathing of females (1.53–1.64 m s^{-1}) than males (1.08–1.56 m s^{-1}). However, the evidence is too limited to conclude any gender difference. After expiration, the air velocity follows an exponential decay over the distance from the mouth [43].

4. Droplet dynamics modeling

4.1. Simplified estimation of droplet falling and evaporation time

When air flow or air convection is not considered, the droplets or aerosol particles are assumed to exist in still ambient air. The diffusion, deposition and evaporation of droplets in still air are well understood and the theories of these processes have been documented in textbooks [44,45]. Vertically, two main forces are exerted on the particle, where the gravity equals the drag force of the air when the terminal settling velocity (V_{TS}) is reached. The approximation of the drag force changes with Reynolds number (*Re*), so does the V_{TS}. The V_{TS} in the Stokes's region ($Re < 1.0$) can be calculated by Eq. (1) [45],

$$V_{TS} = \frac{\rho_p d_p^2 g C_c}{18\eta} \quad [1]$$

where ρ_p is the particle density, d_p is the particle diameter, g is the gravitational acceleration, C_c is the slip correction factor which is important for small particles, and η is the viscosity of air.

The particle V_{TS} in the transition region ($1 < Re < 1000$) is calculated by Eq. (2) and Eq. (3) [45],

$$V_{TS} = \frac{\eta}{\rho_g d_p} \exp\left(-3.070 + 0.9935\, J - 0.0178\, J^2\right) \quad [2]$$

$$J = \ln\left[C_D R_e^2\right] = \ln\left(\frac{4\rho_p \rho_g d_p^3 g}{3\eta^2}\right) \quad [3]$$

where ρ_g is the air density, and C_D is the drag coefficient in Newton's resistance law. In the transition region, C_D has a complicated relationship with *Re*. However, the V_{TS} can be calculated empirically based on the value of $C_D R_e^2$ as shown in Eq. (3).

The evaporation of a pure water droplet is controlled by two competing processes: (a) ambient water vapor arrives and sticks onto the droplet surface, and (b) water molecules evaporate and leave the droplet surface. The complete evaporation time of a water droplet (t_E) in still air is a function of the particle diameter, particle density, temperatures of the droplet and the ambient air, as well as vapor pressures on the droplet surface and in the ambient air [45]. It can be calculated by Eq. (4):

$$t_E = \frac{R\rho_p d_p^2}{8 D_v M\left(\frac{p_d}{T_d} - \frac{p_\infty}{T_\infty}\right)} \quad [4]$$

where R is the gas constant, D_v is the diffusion coefficient of water vapor, M is the molecular weight of water, p_∞ and p_d are the water vapor pressures in the ambient air and on the droplet surface, respectively, T_∞ and T_d are the temperatures of the ambient air and the droplet, respectively.

However, the exhaled droplets contain some solutes. For instance, the major components of mucus include Na^+, Cl^-, K^+, lactate and glycoprotein [46], which would form a droplet nuclei with a diameter of about half of the original droplet size after evaporation [47]. The evaporation time for a droplet to form a nucleus about half of its original size (half evaporation time, $t_{1/2E}$) can be calculated by Eq. (5):

$$t_{1/2E} = \frac{3R\rho_p d_p^2}{32\, D_v M\left(\frac{p_d}{T_d} - \frac{p_\infty}{T_\infty}\right)} = \frac{3}{4} t_E \quad [5]$$

Based on Eqs. (1)–(3), the V_{TS} is about 2.1 m s^{-1} for a 500-μm droplet, 0.25 m s^{-1} for a 100-μm droplet, 3.1×10^{-3} m s^{-1} for a 10-μm droplet, and 3.0×10^{-5} m s^{-1} for a 1-μm droplet. As shown in Fig. 1, the time for a droplet at a height of 1.6 m to fall to the ground varies from 0.78 s for the 500-μm droplet, 6.4 s for the 100-μm droplet, 5.2×10^2 s for the 10-μm droplet, to 5.3×10^4 s for the 1-μm droplet. This clearly indicates that the residence time of a droplet in still air is largely controlled by the droplet size. It is also worth noting that it takes $\geq 5.2 \times 10^2$ s for droplets in the size range of <10 μm to fall onto the ground, which may be sufficiently long for them to be inhaled and lead to significant exposure.

Fig. 1 also shows $t_{1/2E}$ at different values of relative humidity (RH). At a typical indoor RH of 50%, the $t_{1/2E}$ is 0.033 s for a 5-μm droplet, 0.13 s for a 10-μm droplet, and it reaches 13.2 s for a 100-μm droplet and

3.3×10^2 s for a 500-μm droplet. In other words, droplets <10 μm evaporate almost instantaneously, while larger droplets (>100 μm) take a significantly longer time to evaporate. In addition, high ambient RH slows down the droplet evaporation, while low RH accelerates the evaporation. The $t_{1/2E}$ for the same droplet increases by one order of magnitude when RH increases from 0% to 90%. The calculations indicate that, in the still ambient air under typical indoor temperature and RH, large respiratory droplets (>100 μm) settle and fall onto the ground quickly with a limited airborne time (commonly less than a few seconds), while small droplets (roughly <10 μm) evaporate completely and form the droplet nuclei within 1 s. The decrease in size due to the evaporation prolongs the droplet residence time in the air.

4.2. Modeling studies on droplet transport and related dynamics

Several sophisticated models have been applied to simulate the transport and related dynamics of droplets emitted from respiratory activities, as summarized in Table 3. Among them, physical models, mathematical models and Lagrangian models consider several forces acting on the droplets in still ambient air, such as the gravitational force, the drag force, the buoyancy force, etc., and take into account the droplet evaporation in most cases [48–51]. The exhaled air is commonly treated as a turbulent jet with varying initial velocities (ranging from 1 to 50 m s^{-1}) entering the still ambient air. A few other studies have also used computational fluid dynamic (CFD) model or multiphase numerical model (MNM) to simulate the droplet transport with airflow in indoor environment [40,52,53], as well as in public transport [22,23,54].

4.2.1. Modeling studies on droplet dynamics in still air

When the air is exhaled in a horizontal direction in still air condition, the droplet dynamics can be simplified into evaporation, vertical falling, and horizontal travel, which are heavily influenced by the droplet size, the initial air velocity and RH. As illustrated in Fig. 1, the evaporation rate is controlled by droplet size, with small droplets evaporating rapidly to form dried nuclei and large droplets evaporating slowly. Note that there is no absolute division for small and large droplets as it is also influenced by environmental factors (temperature, RH, etc.).

Vertically, large droplets fall onto the ground quickly because of gravity [21,50]. Small droplets have a low gravitational falling velocity, and the reduction in size due to rapid evaporation helps them to remain suspended in the air for a longer time. This results in different removal mechanisms for small and large droplets, i.e., large droplets are mainly removed by gravitational deposition, while small droplets are mainly removed by room air exchange [52]. In addition, high RH slows the evaporation rate and thus promotes the gravitational falling [50].

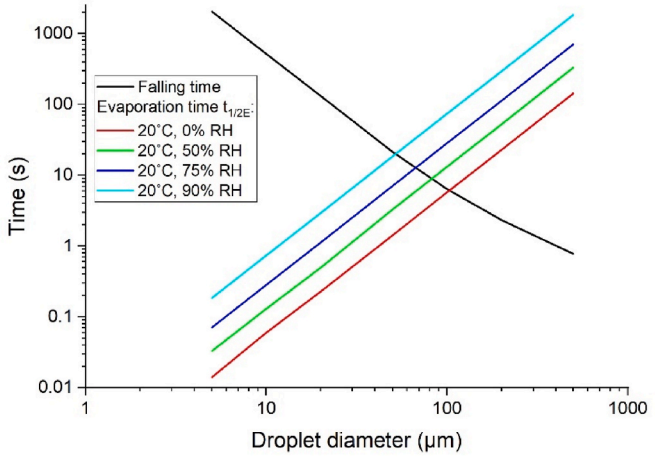

Fig. 1. Droplet falling time (at a height of 1.6 m) and evaporation time to be half of its original size ($t_{1/2E}$) as a function of the diameter. Note that the falling time here only applies to droplets with zero initial vertical velocity in still air, and the interaction between evaporation and gravitational settling is not considered.

On the other hand, horizontal travel distance in still air is influenced by both the initial air velocity and the droplet size. Xie et al. [51] found a great increase in the horizontal travel distance of droplets of 60–100 μm with increasing initial velocity: >6 m for sneezing (v_0 of 50 m s^{-1}), >2 m for coughing (v_0 of 10 m s^{-1}), and <1 m for breathing (v_0 of 1 m s^{-1}). Similarly, Li et al. [49] found that droplets of 50 μm could travel 0.6 m (v_0 of 10 m s^{-1}) or 1.8 m (v_0 of 40 m s^{-1}) horizontally before falling on the ground. The varying behavior of droplets with different sizes is schematically depicted in Fig. 2. As quoted from the study of Chen et al. [48]: "The medium size group (75–400 μm) would be dominated by gravity, falling rapidly to the ground", and travel the shortest distance (~0.6–1.1 m); "the small size group (<75 μm) would follow the air stream, being widely dispersed"; and "the very large size group (>400 μm) would be dominated by inertia and travel a longer distance". In other words, with the same v_0, medium sized droplets (ca. 75–400 μm) tend to travel a short distance horizontally. The distinct behaviors of droplets in the exhaled jet can be explained by the relaxation time (the time required for a droplet to adjust its velocity to new forces), which is proportional to the square of the diameter [45], e.g., 3.1×10^{-4} s, 3.1×10^{-2} s and 6.7 s for droplets of 10 μm, 100 μm and 1500 μm, respectively. Therefore, small droplets quickly follow the exhaled air stream while very large droplets tend to maintain their own velocity. Moreover, while high RH promotes the gravitational falling, it also leads to a longer horizontal travel distance in still air [50].

As demonstrated above, large, medium and small droplets have different transport and dynamic patterns. Assuming a typical scenario with two persons facing each other at a short distance, questions arise as to whether this scenario causes the exposure to expiratory virus-laden droplets? If yes, which droplet size and initial velocity (corresponding to different expiratory activities) contribute to the greatest exposure? Chen et al. [48] specifically studied the relative importance of two exposure routes: (1) the large droplet route (droplets are directly deposited on the membranes of the mouth, nose and eyes) and (2) the short-range airborne route (droplets or nuclei are inhaled in the short-range). They found that the short-range airborne route is dominant at most of the distances for both talking and coughing, while the large droplet (>100 μm) route dominates only at a very close distance (0.2 m for talking, or 0.5 m for coughing).

4.2.2. Modeling studies on droplet dynamics considering room air flow

When the room air flow is considered, the horizontal and vertical travel behaviors of droplets are similar to those in still air condition, e.g., longer horizontal travel distance with larger initial velocity [49], and higher gravitational settling velocity for large droplet sizes [52]. However, the droplets are additionally influenced by the indoor air flow. The influence is greater for small droplets than large droplets as the small droplets tend to follow the air flow even at high air exchange rate (AER). Chao et al. [52] modeled the distribution and transport of droplets in a hospital ward with a ventilation system having both air supply and air return grilles on the ceiling and air changes per hour (*ACH*) of 6 and 11.6, respectively. Droplets <45 μm tend to follow the ventilation flow, and can be airborne pathogen carriers [52].

4.2.3. Modeling studies on droplet dynamics in public transport

Modeling studies on dynamics of respiratory droplets in public transport are presented in Table 4. The ventilation system greatly influences the droplet dynamics. Zhu et al. [23] studied droplet dispersion patterns from four bus ventilation systems with the same air supply rate of 0.54 m^3 s^{-1}. Among them, three are mixing ventilation systems (air supply on the side of ceiling, and air return in the middle of the ceiling or the backwall), and the fourth is a displacement ventilation system (air supply near the bottom of the sidewalls and air return on the side of the ceiling). With displacement ventilation, the exhaled air from the

Table 3
Model studies on droplet transport and related dynamics.

Model type	Model description	Initial velocity (v_0)	Results	Reference
Physical model	Accounting for gravity, drag force and evaporation; using a Turbulent Jet Model.	breathing: 1, 2.5 and 5 m s^{-1}; coughing/sneezing: 10, 20 and 50 m s^{-1}	(1) Droplets of 20 μm from breathing evaporate rapidly, travel 1.0–2.5 m horizontally and fall 0.5–2 cm. (2) Droplets of 40 μm from coughing or sneezing travel about 5–16 m horizontally and fall 4–20 cm. (3) Higher RH slows the droplet evaporation rate, leading to longer falling and horizontal travel distance.	Wang et al., 2005 [50]
Physical model	Accounting for gravity, buoyancy, drag force and evaporation; using an empirical non-isothermal jet theory.	breathing: 1 m s^{-1}; talking: 5 m s^{-1}; coughing: 10 m s^{-1}; sneezing: 20–50 m s^{-1}	(1) Small droplets evaporate rapidly and remain airborne while large droplets (>60–100 μm) fall onto the ground. (2) The exhaled air velocity determines the horizontal travel distance of large droplets (60–100 μm): >6 m (sneezing), >2 m (coughing) and <1 m (breathing). (3) Higher RH increases falling distance for droplets of all sizes, and increases horizontal travel distance only for droplets <40 μm.	Xie et al., 2007 [51]
Lagrangian model	Accounting for gravity, buoyancy, drag force, pressure gradient force, virtual mass force and Brownian diffusion.	10 and 40 m s^{-1}	(1) 1-μm droplets do not travel far in still air due to the rapid decrease in the velocity. (2) 50-μm Droplets could travel 0.6 m (v_0 = 10 m s^{-1}) or 1.8 m (v_0 = 40 m s^{-1}) before falling onto the ground.	Li et al., 2012 [49]
Mathematical model	Accounting for droplet evaporation and dispersion; using using classic jet formulas; focusing on a short-range (2 m) exposure via large droplet route and airborne route.	speaking: 3.7 m s^{-1}; coughing: 11.7 m s^{-1}	(1) Droplets >400 μm travel >2 m. (2) Droplets of 75–400 μm travel the shortest distance (<2 m) and fall onto the ground rapidly. (3) Droplets <75 μm follow the air stream and be widely dispersed. (4) Regarding exposure, the airborne route is more important than the large droplet route.	Chen et al., 2020b [48]
CFD[a] and drift flux model	Accounting for indoor airflow, particle gravity, and particle diffusion; no droplet evaporation.	breathing: 6 m s^{-1}; coughing/sneezing: 20 and 100 m s^{-1}	Droplets of 1 μm travel about 0.5, 3 and > 5 m for v_0 = 6, 20 and 100 m s^{-1}, respectively.	Zhao et al., 2005 [53]
CFD and Lagrangian model	Accounting for indoor airflow, particle gravity, drag force, and pressure variance force; no droplet evaporation.	coughing: 22 m s^{-1}	(1) Droplets ≤30 μm transport with the indoor air flow field. (2) Droplets of 50–200 μm fall by gravity as the airflow slows down. (3) Droplets >300 μm fall slightly and travel almost straightly due to great inertia.	Zhu et al., 2006 [40]
MNM[b] and Lagrangian model	Accounting for indoor airflow, gravity, drag force, basset force, fluid pressure gradient force and droplet evaporation; under unidirectional downward and ceiling-return type ventilation.	10 m s^{-1}	(1) Droplets ≤45 μm settle in <20 s in unidirectional downward flow and in 32–80 s in ceiling-return flow. (2) Droplets >45 μm settle in <6 s in both airflow patterns. (3) Horizontal travel of droplets is < 0.31 m in unidirectional downward flow. (4) Horizontal travel for small droplets covers the whole width of room (2.4 m) in ceiling-return flow.	Chao and Wan, 2006 [38]
MNM and Lagrangian model	Accounting for indoor airflow, particle gravity, drag force, thermophoretic force and Brownian diffusion; no droplet evaporation; in a hospital ward with ceiling-mixing-type ventilation.	coughing: 10 m s^{-1}	(1) Droplets ≤45 μm tend to follow the ventilation flow in lateral dispersion. (2) Droplets >87.5 μm are predominately removed through deposition (95%), mostly in less than 36 s (3) The removal through gravitational settling becomes more important than air exchange with the increasing droplet size.	Chao et al., 2008 [52]

[a] CFD: computational fluid dynamic.
[b] MNM: multiphase numerical model.

infection source moves upwards immediately to the air return outlet without dispersion in the bus cabin, thus minimizing the exposure to the other passengers. In contrast, with mixing ventilation, the air trajectory within the bus is much longer. The infection risk is lower in the displacement ventilation (~0.05%) than the mixing ventilation (0.05%–10.1%). In addition, the infection risk also depends on the location relative to the infection source, the receptor and the return outlet [23]. Regarding natural ventilation by opening of windows or hatch, Ho and Binns [24] found that simultaneous opening of windows that are separated from each other induces through-flow condition in a moving bus, and leads to low exposure. In contrast, opening multiple windows in a stationary bus with bus's mechanical ventilation system turned off induces turbulence and well-mixing of droplets, and is less optimal than opening only one window in front of the index case (sneezer) [55].

The locations of air supply and return also influence the within-bus air flow, and there can be regions with higher or lower droplet concentrations in the bus. For instance, a common arrangement of air supply on both sides of the ceiling and air return in the front of the ceiling results in higher exposure for passengers in front rows [56]. In another case where air supply is at the rear of the ceiling and air return is in the middle of the ceiling, the seats in the back of the bus are in the low-risk region [57]. The seating of the index case and other passengers relative to the air supply and return is an important factor influencing the infection risk. Ooi et al. [58] found that the neighboring passengers downwind of the cougher are typically at a higher risk than the other passengers. When the infection source is near the return outlet, the infection risk for other passengers decreases [23].

Temperature and RH influence the droplet dynamics in the bus as well. One study found that outdoor temperature influences the temperature distribution, and subsequently affects the droplet diffusion speed in the bus cabin [57]. Higher RH slows droplet evaporation and promotes deposition, thereby lowering the risk of droplet transmission [56].

The modern high speed trains often use an up-to-down air conditioning scheme, with the air supply on the ceiling or the sidewall below the luggage rack, and air return at the bottom of the side wall [59]. The type and location of the air supply diffusers affect the cabin air flow, and the dispersion pattern for gas and particles are different under the same

ventilation condition [59]. The through flow within the cabin from the front door to the back door of the train cabin was observed in one study, which significantly promoted the droplet removal ability but also led to much longer dispersion distance [60]. The size of droplets influences the dispersion pattern. Droplets <36 μm can be dispersed throughout the cabin while droplets >87.5 μm deposit mostly near the seat of the emitter [61].

Compared with other types of public transport, the airplane cabin has a high efficiency particulate air filter (HEPA) system to purify the cabin air. The air supply is commonly located on the ceiling and the return outlet on the bottom sidewall. The transport of droplets or droplet nuclei is highly influenced by the airflow, which can vary between different cases. Gupta et al. [22] modeled the transport of respiratory droplets in an aircraft cabin using a CFD model. For the specific airplane cabin scenario (seven-row and twin-aisle, fully occupied, the index patient sits in the middle of the cabin, *ACH* of 33.7, air supply inlets on the top wall, air outlets at the bottom of the sidewalls), most of the droplets were transported within one row from the index patient in 30 s, and the droplets were reduced to 12% after 4 min due to the removal by air exchange. In another study by Talaat et al. [54], the aerosol transmission in an aircraft cabin with and without sneeze shield between passengers was modeled. The results indicate that the droplets start to spread in 10 s to other individuals, and in 2–3 min, all droplets are removed by ventilation or deposition. Using sneeze shields between passengers can effectively redirect part of local air to the back of front seats and reduce the aerosol transmission. For a comprehensive understanding on the ventilation and airplane cabin air quality, refer to the review by Elmaghraby et al., in 2017 [62].

5. SARS-CoV-2 transmission in public transport

A previous review by Browne et al. [6] summarized the research on influenza and coronavirus transmission in transportation and transportation hubs, which included 41 studies ranging from air transport (airplane cabin), sea transport and ground transport. Herein, we focus on the transmission of SARS-CoV-2 in bus, train and airplane, mostly based on epidemiological studies.

5.1. Bus

Table 5 provides an overview of the SARS-CoV-2 transmission studies in bus and train. SARS-CoV-2 virus has been detected both on the surfaces and in the air of transit buses in Barcelona, Spain [64], Tehran, Iran [65] and Apulia, Italy [66]. However, the presence of SARS-CoV-2 in transit buses was not found in Chieti, Italy [67], where strict rules were adopted for passengers including wearing face masks, distancing, hand hygienization as well as opening the bus windows. In contrast, wearing face mask and distancing were required in the study of Apulia, Italy [66], while no such information was provided in the other two studies of Barcelona and Tehran.

Relatively high transmission rates (estimated as the percentage of new cases in the total population) of 17% [9], 35% [10], 44% [68], and 92% [69] were repforted on coach/tour buses. The first study by Luo et al. [9] investigated COVID-19 transmission in buses in Hunan, China in January 2020. Specifically, a COVID-19 infection source (patient A) took a 2.5-h ride on one coach bus (all 49 seats occupied) and a 1-h trip on a minibus (12 of 18 seats occupied). The windows were closed on both buses with ventilation systems on. In total, patient A infected eight persons on the coach bus and two on the minibus. The majority of infected persons were located more than 2 m away from the infection source, indicating potential aerosol transmission. Another report [10] described a case study on the buses in Zhejiang, China in January 2020. A source patient infected 24 people on the same bus during a 2.5-h bus tour, where the bus ventilation system was operated in an indoor-recirculation mode. The highest transmission rate of 92% was observed on a coach bus carrying 52 passengers from Greece to the Middle East over an 8-day trip with 10 h of driving per day [69].

In contrast, zero transmission was reported in school buses in Virginia, USA [70]. Using public transport in Zurich, Switzerland did not lead to significant differences in contracting COVID-19 among health care workers in a local hospital [71].

Overall, current literature points to high transmission rates on coach or tour buses, which can be attributed to the insufficient ventilation [18] and prolonged time of close contact among passengers (ranging from a few hours to a few days). Based on very limited evidence, it appears that the use of transit bus or school bus is associated with much lower transmission risk, which might be explained by the wearing of face mask, shorter riding duration and frequent opening of bus doors. On the other hand, epidemiological study on city transit bus may be more challenging as it is difficult to collect the riding information and trace the passengers.

5.2. Subway and train

Hu et al. [12,72] studied the transmission rate of COVID-19 on high-speed trains in China between December 19, 2019 and March 6,

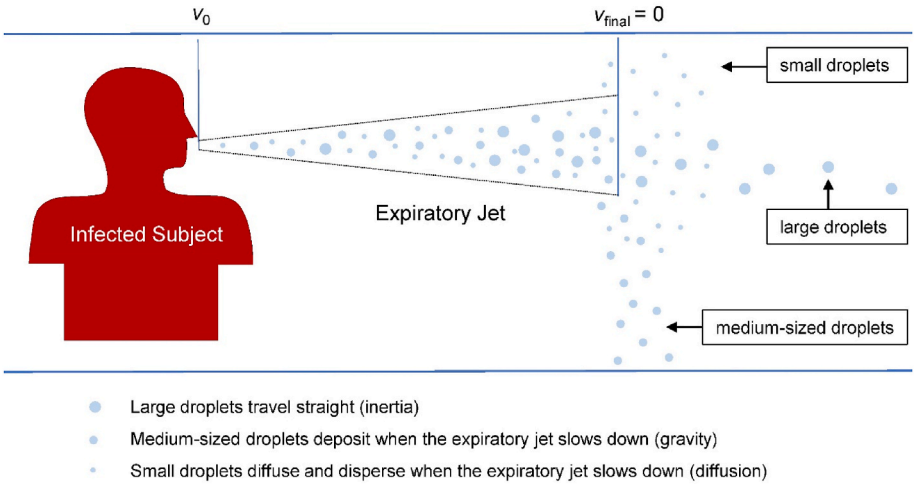

Fig. 2. Schematic illustration of dynamics of droplets with different sizes emitted from an infected subject. The droplet trajectory can also be influenced by air temperature, RH, initial expiratory jet velocity, etc. As a result, there are no definite size ranges for large, medium and small droplets, which can vary from case to case.

Table 4
Modeling studies on respiratory droplet dynamics in public transport and associated transmission risk.

Public transport	Model	Ventilation condition	Results	Reference
Bus	CFD and Wells-Riley model	3 mixing ventilation (MV) and 1 displacement ventilation (DV) systems; $ACH = 57.6$	(1) Exhaled air in MV have longer trajectory than in DV. (2) Lower airborne infection risk in DV (~0.05%) than MV (0.05%–10.1%).	Zhu et al., 2012 [23]
Bus	CFD	air supply on both sides of the ceiling; air return in the front of the ceiling	(1) Higher risk for passengers in front rows. (2) Under higher RH droplets evaporate slower and deposit more quickly, attaining less risk of droplet transmission. (3) >84% of droplets are deposited on bus or body surfaces; 5.6–6.0% are suspending in the air; 1.3%–10.4% are removed from the air return.	Yang et al., 2020 [56]
Bus	CFD	air supply on the rear of the ceiling; air return in the middle of the ceiling	(1) Higher outdoor temperature leads to lower droplet diffusion speed. (2) The seats in the back of the bus belong to the low-risk region.	Duan et al., 2021 [57]
Bus	CFD	opening of windows at stationary and moving conditions	(1) When stationary, turning on the heater induced the well-mixing condition and leads to higher exposure; (2) When moving, opening of windows that are separated from each other induces through-flow condition, leading to low exposure.	Ho and Binns, 2021 [24]
Bus	CFD and AI	Air velocity of 0.1 m s^{-1} from supply vent	(1) The droplets <250 μm remain suspended in air and be transferred to other parts of the bus. (2) 59% of the initial droplets are deposited within 2 m, and droplet concentration declines to 87% at 3 m.	Mesgarpour et al., 2021 [63]
Bus	CFD and measurement	3.6 m s^{-1} from supply vent; 1.9 m s^{-1} from supply vent	The neighboring passengers down-wind of the cougher are typically at a higher risk than the other passengers.	Ooi et al., 2021 [58]
Bus	CFD	Ventilation off in a stationary bus; different sets of windows opened	(1) Opening the window next to the index case leads to high exposure to the front. (2) Opening the windows in the front row reduces the exposure. (3) Opening multiple windows leads to well-mixing of droplets in the bus, and is not the optimal option.	Yao and Liu, 2021 [55]
Bus	CFD and mass balance model	1.7 and 3.2 L s^{-1} per person	Airborne transmission was the dominant route (16.3% and 11.2%) while fomite transmission risk was negligible (3.1×10^{-6} and 4.7×10^{-5}).	Cheng et al., 2022 [18]
High speed train	CFD	air supply on the ceiling (0.046 m s^{-1}); 4 different outlet cases	(1) The through flow and back door exhaust (case 3) has the highest droplets removal ability but also the longest dispersion distance. (2) The no through flow and lower exhaust (case 2) shows the minimum impact to other passengers.	Zhang and Li, 2012 [60]
High speed train	CFD	4 types of air suppy diffusers on the sidewall or ceiling; outlets on the bottom of sidewalls	(1) Gas and particle show different dispersion patterns with the same diffisuer. (2) Diffuser type 1 is best in restricting gas from dispersing to other passengers. (3) Diffuser type 2 and 3 lead to smaller average particle volume fraction in breathing zone.	Yang et al., 2018 [59]
KTX-Sancheon train	CFD	Air supply (55 m^3 min^{-1} $cabin^{-1}$) below the window, air outlets on the side and floor	(1) droplets <36 μm follow the air flow; droplets 36–45 μm deposite on nearby passengers; droplets >62.5 μm deposite near the emitter. (2) The deposition fraction increases with droplet diameter.	Ko et al., 2019 [61]
Airplane (twin aisle cabin)	CFD and Lagrangian method	air supply on the middle of the cabin ceiling and air return on the bottom of side wall; $ACH = 33.7$	(1) Most of the droplets are transported within one row from the index patient in 30 s, and up to 7 rows in 4 min (2) Total airborne droplets were reduced to 48%, 32%, 20% and 12% of the initial concentrations after 1, 2, 3, and 4 min, respectively.	Gupta et al., 2011 [22]
Airplane (single-aisle cabin)	CFD	air supply on the top of side wall and the air return on the bottom of side wall; Air supply: 566 L s^{-1}	(1) Droplets start to be transmitted to other individuals in 10 s and be transported to the other side of the plane in 50 s (2) Exhaled droplets are removed from the air in 2–3 min, with 21–26% being removed by ventilation and the majority depositing on surface. (3) Using sneeze shields between passengers educes the aerosol transmission.	Talaat et al., 2021 [54]

2020. A total of 2334 COVID-19 patients and 72093 close contacts who had co-travel time of 0–8 h on the same high-speed trains were quantified. The transmission rate for train passengers on seats within 3 rows and 5 columns from the index patient averaged at 0.32% (range: 0–10.3%). Passengers sitting in the same row had a transmission rate of 1.5%, higher than those sitting in other rows (0.14%). Passengers adjacent to the index patient had the highest transmission rate of 3.5%. The transmission rate increased by 0.15% per hour of co-travel. However, no information of air ventilation and filtration was reported in this study.

Increased subway ridership was associated with higher COVID-19 infection rate or mortality in New York city [73–75], although another study in New York city did not find such an association [76]. The prevalence of using the subway system during the COVID-19 pandemic and lockdown period was higher for those performing essential work or without private vehicles, also reflecting socioeconomic disparities among the New York residents. More studies are needed to justify whether the association in New York city applies to other regions.

5.3. Airplane

Table 6 lists the 22 studies on COVID-19 transmission and/or prevalence on airplanes. Among them, 13 studies reported in-flight transmission rates ranging from 0% to 10% with a median of 0.36% [7,12,77–87]. The highest transmission rate of 10% was reported on a domestic flight in Japan where 14 passengers were infected [87]. However, it may be overestimated because the secondary cases belonged to two family clusters and in-family transmission after the flight may have occurred. On a flight from London, UK to Hanoi, Vietnam on Mar. 1–2, 2020, 16 out of 217 passengers were infected with a transmission rate of 7.3% [80]. A transmission rate of 4.6% was reported by Swadi et al. on a flight from Dubai, UAE to Auckland, New Zealand [7]. Zero in-flight transmission rate was reported on a commercial flight from Wuhan to Toronto [82], on a repatriation flight from Japan to Israel for Diamond Princesses passengers [81], and on two flights from Wuhan to Thailand [83]. Pang et al. [84] reported very low transmission rates of 1.4×10^{-6} – 1.3×10^{-7} on a global scale, but this result was likely underestimated.

First, only the infected cases from English literature and media were searched (bias due to unreported cases and reports in other languages). Second, epidemiological tracing of the index cases and secondary cases from the flight is necessary for an accurate estimation of the transmission rate. Unfortunately, only 13 epidemiological studies were used compared with hundreds of thousands of flights that were included for analysis.

Some studies reported COVID-19 cases on flights but had neither concrete evidence for in-flight transmission nor a transmission rate [8,88–91]. Other studies reported only COVID-19 prevalence (0–8.3%, indicating the proportion of a population who are infected with SARS-CoV-2) in the origin city/country but not the in-flight transmission [92–95].

High transmission rates occurred at close distance, e.g., 3.8% for those sitting within two rows from the index case compared to an overall transmission rate of 0.2% [78], and 9.2% for those sitting adjacent to the index case compared to an overall transmission rate of 0.33%−0.60% [12]. Swadi et al. [7] found that all the infected cases were seated within two rows and two columns away from the index case. A transmission rate of 100% (12 infection cases) was also reported within a business class cabin [80]. Wearing face mask may have influenced the in-flight transmission rates. In four cases with relatively high transmission rates (4.6%, 5.6%, 7.3% and 10%) [7,80,86,87], wearing face masks was not mandatory or only partially followed. No association between the flight duration and the transmission rate can be observed from the reviewed studies.

In airplanes, fomite transmission (through polluted surface) is also a potentially important route [96]. The contaminated surfaces in aircraft cabin include high-touch surfaces such as aisle seatback and toilets. On a 5- to 6-h flight, all touchable surfaces are contaminated [97]. Using onboard toilet may have been responsible for one case of in-flight transmission of COVID-19 from Milan, Italy to South Korea where strict infection control measures were implemented [77].

6. Factors influencing the behavior of (virus-laden) droplets

6.1. Temperature and RH

Casanova et al. [98] studied the survival of two surrogate viruses for SARS-CoV, the transmissible gastroenteritis virus (TGEV) and mouse hepatitis virus (MHV), on the surface of stainless steel. They found that the most rapid inactivation occurred at 40 °C, followed by 20 °C, while the slowest inactivation was at 4 °C. Similarly, Prussin et al. [99] showed that under 75% RH, the infectivity of the enveloped bacteriophage Phi6 virus in droplets on surface decreased exponentially as temperature increased from 14 °C to 34 °C. Low temperature appears to favor the survival or infectivity of the tested viruses. In contrast, the effect of RH is more complicated. Greater survival rates (the percentage of virus still alive after a given period of time) on surface were observed for TGEV and MHV at either low RH (20%) or high RH (80%) than at moderate RH (50%) at 20 °C [98]. This U-shape relationship between RH and virus survival rates at room temperature (20–24 °C) was also reported for two bacteriophages (MS2 and Phi6) on surface and as aerosol [100] and Influenza A virus on surface [101]. For the bacteriophage Phi6 in droplets, the infectivity showed the same U-shape RH dependency at 25 °C and 37 °C with relatively low infectivity at intermediate RH range (~60%–85%), but remained high across all RHs at 14 °C and 19 °C [99].

RH also influences the evaporation of droplets as discussed in Sect. 4.1. High RH leads to slower evaporation, and higher deposition fraction of droplets on both human body and the ground, while lower RH triggers evaporation, leading to the reduction of droplet sizes and longer time suspended in the air [102]. In other words, low RH favors the airborne transmission. It is recommended to keep the indoor RH in the range of 40%–60%, which lowers the virus survival rate and infectivity, reduces the risk of airborne transmission, and is also comfortable to humans [103].

6.2. Air flow pattern

The indoor air flow pattern plays a key role in determining the transport of particles, especially for aerosol particles <40 μm. According to different ventilation systems, a variety of air flow patterns exist, with common ones including unidirectional downward flow (supply vents on the ceiling and return vents on the floor), ceiling-return type flow (both the supply and return vents on the ceiling), and unidirectional upward flow (air supply at the floor level and air return on the ceiling).

Under unidirectional downward air flow, droplets <45 μm tend to follow the unidirectional downward bulk air stream with a vertical settling time of 15–20 s, while droplets of 87.5 μm and 137.5 μm deposit in around 5 s and 3 s, respectively [38]. The horizontal travel distance for droplets is limited to 0.31 m. It must be noted that such influence can be very case-specific, as the particle dynamics can also be affected by the temperature distribution, the relative locations between the infection source and susceptible subject, the initial droplet velocity as well as the indoor air flow pattern. For instance, when two persons are facing each other within 1.0 m in a room with unidirectional downward ventilation, the vortex airflow around the human body is formed by the combination of downward ventilation flow and the upward human thermal plume (HTP). In such a case, 100-μm droplets disperse mainly within the HTP zone, and cannot be carried out to the susceptible subject (1.0 m apart), while a part of 10-μm droplets can be dispersed around the susceptible subject [39].

Under the ceiling-return type of airflow, the droplets first transport downward due to gravity and the downward airflow stream, and then are separated into two paths depending on the size. Large droplets continue to settle downward and deposit on the floor, while small droplets follow the airflow stream and move upward to the air return vents. In addition, the horizontal dispersion of droplets <45 μm is across the whole room width (2.4 m) [38], which is much greater than in the case of unidirectional downward flow or still air condition [53].

Under the unidirectional upward air flow, which is also associated with displacement ventilation, the temperature difference between exhaled air and ambient air was smallest in the upward air flow, which caused the exhaled air to rise less vertically than in the mixing ventilation or without ventilation conditions [43]. As discussed earlier in Sect. 4.2.3, with the displacement ventilation in the bus, the trajectory of the exhaled air from the index person is the shortest compared with the other three mixing ventilation systems, leading to a potentially lower transmission risk [23]. Moreover, it is commonly acknowledged that higher ventilation rates can reduce the risk of disease transmission in confined spaces [104,105]. A study using a numerical model (based on Wells-Riley model) showed that the reproduction number (R_A) of influenza reduced from 2.22 to 1.17 by doubling the ventilation rate in the train cabin from 13 h^{-1} to 26 h^{-1} [105].

6.3. Wearing face masks

The use of personalized protection equipment (PPE, such as face mask) is a common measure against virus transmission in public transport around the world. Several recent studies have measured the efficiency of the face mask in filtering particles without accounting for the leakage under normal wearing scenarios. Relatively low filtration efficiencies (5%–25%) were observed for fabric face masks under realistic pressure drops and air velocities [106–109]. The filtration efficiencies vary with the types of materials and the number of layers used in the masks. For example, Zhao et al. [109] reported filtration efficiency of 5%–25% for common fabrics of cotton, polyester, nylon and silk, 6%–10% for polypropylene spunbond, and 10%–20% for paper-based products. Hill et al. [106] reported a filtration efficiency of 17.4% for masks with a single layer cotton, but much higher value (>98%) for N95/PN95 masks.

Under normal wearing scenarios with imperfect fitting, gaps between the mask and face can lead to leakage of air upon inhalation or

Table 5
Summary of SARS-CoV-2 transmission in the bus, train and subway.

Method	Public transport	Location/ Flight information	Protective measures	Exposure condition	Virus detection rate[a]/Transmission rate[b]	Reference
Measurement study	Transit bus	Chieti, Italy	hand and surface disinfection, face mask; distancing	NA[c]	0.0%	Di Carlo et al., 2020 [67]
	Transit bus, subway	Barcelona, Spain	NA	NA	37% (more common on the surface than in the air)	Moreno et al., 2021 [64]
	Airport, transit bus, subway	Tehran, Iran	NA	NA	67% (80% in the airport, 50% in subway stations, 100% in subway trains and 50% in buses)	Hadei et al., 2021 [65]
	Transit bus, train	Apulia, Italy	Face mask, distancing	NA	19.3% in buses; 2% in trains	Caggiano et al., 2021 [66]
Epidemiological study/Case study	Coach bus, minibus	Hunan, China	one wore face mask on minibus	One index patient took one coach bus (2.5 h) and one minibus (1 h).	17% (8/48 on the coach bus, and 2/12 on the minibus)	Luo et al., 2020 [9]
	Coach bus	Zhejiang, China	No	One index patient took a round 100-min bus trip and participated a 150-min worship event.	35% (24/67); no significant difference between high-risk zone (<2 m) and low-risk zone (>2 m)	Shen et al., 2020 [10]
	Tour bus	Hokkaido, Japan	Face mask	4-day tour	44% (18/41)	Tsuchihashi et al., 2021 [68]
	School bus	Virginia, USA	Face mask, Natural ventilation	Students were transported by school buses at near full capacity.	0%	Ramirez et al., 2021 [70]
	Public transport	Zurich, Switzerland	Face mask	healthcare workers (HCW) in a hospital investigated for possible route of transmission	NA (Using public transport did not lead to higher COVID-19 infection rate among HCW)	Steinwender et al., 2021 [71]
	Coach bus	Greece – Middle East	NA	8-day tour, 10 h/day of driving in a religious tour	92% (48/52)	Vlacha et al., 2021 [69]
	Train	China	NA	2334 COVID-19 patients and 72093 close contacts were analyzed on high-speed trains in China during Dec. 2019–Mar. 2020.	0.32% for passengers sitting within 3 rows and 5 columns from the index case; 1.5% for the same row; 3.5% for adjacent to the index case	Hu et al., 2021 [12]
	Subway	New York City, USA	NA	NA	NA (increased subway use associated with higher COVID-19 rate with a RR of 1.11)	Sy et al., 2020 [75]
	Subway	New York City, USA	NA	NA	NA (high COVID-19 inequity index associated with higher subway ridership, and associated with higher COVID-19 mortality)	Carrion et al., 2021 [73]
	Subway	New York City, USA	NA	NA	NA (The subway ridership (turnstile entry data) and COVID-19 deaths and cases were highly correlated)	Fathi-Kazerooni et tal., 2021 [74]
	Subway	New York City, USA	NA	NA	NA ("no evidence that subway ridership was related to the COVID-19 infection rate")	Hamidi et al., 2021 [76]

[a] For measurement study.
[b] For epidemiological study/Case study.
[c] Not available.

exhalation. The effective filtration efficiency (η_e) of a face mask considering leakage can be expressed as:

$$\eta_e = \eta\left(1 - \frac{Q_l}{Q_s}\right) \quad [6]$$

where η is the nominal filtration efficiency, Q_s is the total inhaled or exhaled air flow and Q_l is the leaked air through the gaps [110], although Q_l is difficult to measure. Reported η_e values for surgical face mask from measurement ranged from 40% [111] to 74%–80% [112].

Despite their relatively low filtration efficiency, surgical face masks can significantly reduce the emissions of human corona virus and influenza virus. Leung et al. [113] detected human seasonal coronavirus (not SARS-CoV-2) in 3 of 10 (30%) respiratory droplet samples and in 4 of 10 (40%) aerosol samples without face masks, but 0% with surgical face masks. Heald et al. [114] found that wearing face coverings in public transport and retail outlets in UK reduced the infection risk of COVID-19 by 9%. In a train with 150 passengers and an *ACH* of 13, wearing face masks (with filtration efficiencies assumed to be 40% and 97%) by susceptible people reduced the R_A value from 2.22 to 2.08 and 1.13, respectively. Moreover, a modeling study using Wells–Riley equation demonstrated that when ordinary medical surgical masks with a filtration efficiency of 50% were worn by both the infector and the susceptible person, an infection probability of <1% in confined spaces could be achieved at a much smaller ventilation rate (25%) compared to the case without wearing face masks [104].

A recent review by Freedman and Wilder-Smith [115] focused on the effectiveness of face masks in airplanes and concluded that the strict use of face masks appeared to be protective. More recently, Cheng et al. [116] used a single-hit model of infection and demonstrated that the effectiveness of face masks in mitigating the SARS-CoV-2 transmission was influenced by the regimes of virus abundance. Under virus-rich regime (e.g., virus concentration is 100 times of the 50% infection dose), wearing face masks cannot effectively lower the infection probability. In contrast, under virus-limited regime (e.g., virus concentration is equivalent to or lower than the 50% infection dose), wearing face masks can lead to a substantial reduction in the infection probability.

7. Conclusions and Outlook

Along with the worldwide spread of COVID-19, there has been a debate on the main transmission route of COVID-19 in indoor environment and public transport. Fundamental understanding of the emissions

and dynamics of expiratory virus-laden droplets and the consequent exposure routes to the virus is necessary for taking effective control measures. Here, we conducted a review of the related literature aiming to provide a broad overall view on the atmospheric behavior of the respiratory virus-laden droplets. Due to limited time and space, the literature review is limited to the databases of Web of Science and PubMed. Specifically, this review summarizes (1) the emission profiles of the droplets from different respiratory activities, including emission rates, size distributions and initial velocities; (2) the dynamics of droplets in indoor environment; (3) the infection risk of COVID-19 in public transport; and (4) the factors influencing the virus transmission. Main conclusions and perspectives are as follows.

(1) A considerable number of droplets in both super-micron and submicron size ranges are emitted from human respiratory activities, except breathing which produces droplets mainly <1.0 μm. Droplet size and number as well as the exhaled velocity vary between different respiratory activities. However, the data are from a limited number of studies, and the emission profiles vary substantially for the same respiratory activity. The interpersonal variability and vocal loudness could explain some of the variation. Super emitters have been identified who emit significantly more droplets (by orders of magnitude) than others. However, there is a lack of a standardized test protocol, and the instruments applied in the studies focus on different size ranges (e.g., >10 μm

Table 6
Summary of SARS-CoV-2 transmission in airplanes.

Flight	Protective measures	Exposure condition	Transmission rate[a]/prevalence rate[b]	Reference
Wuhan–Guangzhou, China–Toronto, Canada	Face mask	A 15-h flight carried 350 passengers, of whom 2 were index patients.	0%	Schwartz et al., 2020 [82]
Japan–Israel	Face mask	A 13.5-h repatriation flight carried 11 passengers who were previously on Diamond Princesses cruise ship.	0% (2 out of 11 were tested positive but may be infected before the flight)	Nir-Paz et al., 2020 [81]
Wuhan – Thailand	NA	two flights, each with one index case	0%	Okada et al., 2020 [83]
Literature review and synthesis of transmission rate	NA	2866 index cases and 44 secondary cases identified from IATA, CDC data base and the published literature.	$1.4 \times 10^{-6} - 1.3 \times 10^{-7}$	Pang et al., 2021 [84]
18 flights from Europe to England	No	NA	0.20% (17/2313) on average; 3.8% within 2 rows from index person	Blomquist et al., 2021 [78]
Milan, Italy – South Korea	N95 face mask	An 11-h evacuation flight carried 299 passengers.	0.30% (one possible in-flight transmission, potentially via the toilet)	Bae et al., 2020 [77]
830 international flights arriving in Beijing	Face mask	161 COVID-19 cases confirmed 94 flights, of which, in-flight transmission observed on 2 flights	0.36% (flight 1); 0.42% (flight 2)	Zhang et al., 2021 [85]
Wuhan – other cities, China	NA	175 COVID-19 index cases among 5797 passengers on 177 flights during Jan. 4–23, 2020	0.33%–0.60% (overall); 0.7% (the middle seat); 9.2% (adjacent to the index case)	Hu et al., 2021 [12]
Boston, USA–Hong Kong, China	NA	A 15-h flight carried 294 passengers.	1.4% (4/294)	Choi et al., 2020 [79]
Dubai, UAE - Auckland, New Zealand	Face mask not mandatory	An 18-h flight carried 86 passengers. 2 persons were likely the index cases in the incubation period when on board.	4.6% (4/86)	Swadi et al., 2021 [7]
Sydney – Perth, Australia	Face mask (sporadic usage)	On a 5-h flight with 213 passengers, 18 primary cases and 11 secondary cases	5.6% (11/195)	(Speake et al., 2020) [86]
London, UK–Hanoi, Vietnam	Face mask not mandatory	A 10-h flight carried 16 crew members and 201 passengers.	7.3% (16 infected, of whom 12 were seated in business class and infected by one symptomatic passenger.)	Kahun et al., 2020 [80]
A domestic flight in Japan	Face mask (65% passenger)	One index case on the flight affected 14 passengers who belong to 2 family clusters	10% (may be overestimated due to in-family transmission)	Toyokawa et al., 2022 [87]
Singapore–Hangzhou, China	Face mask	A 5-h flight carried 335 passengers and 11 crew members, including a tour group coming from Wuhan	NA (one passenger was likely infected during the flight.)	Chen et al., 2020a [88]
Tel Aviv, Israel – Incheon, South Korea	NA	A 11-h flight carried 39 pilgrims to South Korea, of whom, 30 were later diagnosed COVID-19	NA (one cabin crew member was likely infected on board)	Mun et al., 2021 [90]
Bangui, Central African Republic –Yaoundé, Cameroun	NA	One person was diagnosed COVID-19 after returning from a business trip to Africa	NA (possible transmission on the flight)	Eldin et al., 2020 [8]
18 international flights arriving at or departing from Greece	NA	NA	NA (five cases of probable in-flight transmission were observed on one flight from Israel, on which two index cases were identified)	Pavli et al., 2020 [91]
Tel Aviv, Israel–Frankfurt, Germany	NA	A 4.5-h flight carried 102 passengers, of whom, 24 were from a tour group.	NA (2 likely onboard transmissions)	Hoehl et al., 2020 [89]
5 evacuating flights from Wuhan, China to Japan	Yes	symptomatic persons were triaged.	NA (infection prevalence: 8.3% among triaged persons; 0.9% among not triaged persons)	Hayakawa et al., 2020 [92]
17 repatriation flights from Wuhan, China	NA	NA	NA (infection prevalence: 0–1.9%; 0.44% on average)	Thompson et al., 2020 [94]
7 flights to Greece	NA	NA	NA (infection prevalence: 3.6%–6.3%)	Lytras et al., 2020 [93]
Wuhan – Singapore	Surgical masks	An evacuation flight carrying 94 passengers	NA (infection prevalence: 3.2%)	(Ng et al., 2020) [95]

for optical microscope, ~0.7–20 μm for APS, and 0.01–0.43 μm for SMPS), which makes a direct comparison among studies difficult. Future research should work toward a unified testing protocol that covers a wide range of droplet sizes. Considering the variability of droplet emission profiles associated with health conditions, it is also necessary to test the droplet emissions from persons with respiratory symptoms, as most of the reviewed studies recruited healthy subjects only.

(2) Droplet size is one of the most important factors determining the dynamics: large droplets settle quickly and evaporate slowly, while small droplets evaporate quickly to form nuclei before settling down and remain in the air for a prolonged time. The horizontal travel distance of the droplets largely depends on the droplet size together with the initial velocity of exhaled air. Moreover, the droplet dynamics and exposure may be case-specific and are significantly affected by the room air flow pattern related to different ventilation types. Ventilation in circulation mode on the bus may be responsible for the high transmission rate, while the air conditioning system with HEPA filter on the airplane explains the relatively low transmission rate on the airplane. More studies on the influence of ventilation types on droplet dynamics are needed to help fully assess the importance of each transmission route in different circumstances as well as provide a robust scientific basis for the improvement of ventilation systems.

(3) The public transport systems reviewed in the paper (bus, subway, train and airplane) can be an important route in transmitting COVID-19. Based on limited studies so far, the transmission rates in the coach/tour bus (17%, 35.3%, 44% and 92%) were much higher than in a school bus and transit bus, which might be attributed to the differences in the opening of windows or doors, the co-travel (exposure) time and wearing of face mask. Evidence from New York city indicates that higher subway ridership was associated with increased COVID-19 infection rate and mortality. The transmission rates in airplanes were 0–10% (median: 0.36%) and 0.32% in high-speed trains in China. Possible transmission routes include both airborne transmission and short-distance droplet transmission. Larger distance from the infection source and shorter co-travelling time lowered the infection risk, but did not eliminate the chance of infection, as passengers sitting further away (>2 m) were also infected. The fomite transmission (through polluted surface) is also a potentially important route in airplane. The relative importance of each transmission route as well as the transmission rate are largely determined by the droplet dynamics, and therefore depend on the size and initial velocity of the virus-laden droplets, indoor air flow pattern related to different ventilation systems, relative location between the infection source and receptors, etc.

(4) The transmission rate is also affected by the survival rate and the infectivity of the virus. Low temperature favors the survival and infectivity of virus (surrogate virus, not SARS-CoV-2), while the virus is inactivated much faster under high temperatures. In addition, either high (>80%) or low (<20%) RH favors higher virus survival rate. Nevertheless, the knowledge of the environmental influences on SARS-CoV-2 is rather limited, and more studies are urgently needed to better understand the behaviors of the virus.

(5) This review provides the following implications for mitigating the transmission of COVID-19. First, wearing face masks can be an effective way to intercept the droplets and reduce the exposure risk under the low virus abundance (most public places). Second, distancing is also recommended to lower the risk of exposure as higher transmission risk is found within shorter distance in public transport. Moreover, regarding the airborne transmission route, higher ventilation rate and appropriate ventilation types (such as displacement ventilation type, non-recirculation ventilation or recirculation ventilation with HEPA filtration system) should be considered to lower the transmission rate. Proper ventilation systems that can minimize the transmission risk should be a focus of future studies.

CRediT authorship contribution statement

Qiaoqiao Wang: Writing – review & editing, Writing – original draft, Validation. **Jianwei Gu:** Writing – review & editing, Writing – original draft, Investigation, Conceptualization. **Taicheng An:** Writing – review & editing.

Declaration of competing interest

The authors declare that they have no known competing financial interests or personal relationships that could have appeared to influence the work reported in this paper.

Acknowledgments

The study was supported by the National Natural Science Foundation of China (41907182), the National Key R&D Program of China (2018YFC0213901 and 2019YFC1804503), the Fundamental Research Funds for the Central Universities (21621105), the Guangdong Innovative and Entrepreneurial Research Team Program (2016ZT06N263), the Guangdong-Hongkong-Macau Joint Laboratory of Collaborative Innovation for Environmental Quality, and Science and Technology Program of Guangdong Province (2021A0505030070).

References

[1] WHO, WHO Coronavirus, (COVID-10) Dashboard. https://covid19.who.int/, 2022.
[2] R. Zheng, Y. Xu, W. Wang, G. Ning, Y. Bi, Spatial transmission of COVID-19 via public and private transportation in China, Trav. Med. Infect. Dis. 34 (2020).
[3] B. Cazelles, C. Comiskey, B. Nguyen-Van-Yen, C. Champagne, B. Roche, Parallel trends in the transmission of SARS-CoV-2 and retail/recreation and public transport mobility during non-lockdown periods, Int. J. Infect. Dis. 104 (2021) 693–695.
[4] IATA, International Air Transport Association Annual Review 2019, 2019. Seoul.
[5] A.S. Gonzalez-Reiche, M.M. Hernandez, M.J. Sullivan, B. Ciferri, H. Alshammary, A. Obla, S. Fabre, G. Kleiner, J. Polanco, Z. Khan, B. Alburquerque, A. van de Guchte, J. Dutta, N. Francoeur, B.S. Melo, I. Oussenko, G. Deikus, J. Soto, S. H. Sridhar, Y.C. Wang, K. Twyman, A. Kasarskis, D.R. Altman, M. Smith, R. Sebra, J. Aberg, F. Krammer, A. Garcia-Sastre, M. Luksza, G. Patel, A. Paniz-Mondolfi, M. Gitman, E.M. Sordillo, V. Simon, H. van Bakel, Introductions and early spread of SARS-CoV-2 in the New York City area, Science 369 (6501) (2020) 297–301.
[6] A. Browne, S. St-Onge Ahmad, C.R. Beck, J.S. Nguyen-Van-Tam, The roles of transportation and transportation hubs in the propagation of influenza and coronaviruses: a systematic review, J. Trav. Med. 23 (1) (2016).
[7] T. Swadi, J.L. Geoghegan, T. Devine, C. McElnay, J. Sherwood, P. Shoemack, X. Ren, M. Storey, S. Jefferies, E. Smit, J. Hadfield, A. Kenny, L. Jelley, A. Sporle, A. McNeill, G.E. Reynolds, K. Mouldey, L. Lowe, G. Sonder, A.J. Drummond, S. Huang, D. Welch, E.C. Holmes, N. French, C.R. Simpson, J. de Ligt, Genomic evidence of in-flight transmission of SARS-CoV-2 despite predeparture testing, Emerg. Infect. Dis. 27 (3) (2021) 687–693.
[8] C. Eldin, J.C. Lagier, M. Mailhe, P. Gautret, Probable aircraft transmission of Covid-19 in-flight from the Central African Republic to France, Trav. Med. Infect. Dis. 35 (2020) 2.
[9] K. Luo, Z. Lei, Z. Hai, S. Xiao, J. Rui, H. Yang, X. Jing, H. Wang, Z. Xie, P. Luo, W. Li, Q. Li, H. Tan, Z. Xu, Y. Yang, S. Hu, T. Chen, Transmission of SARS-CoV-2 in public transportation vehicles: a case study in Hunan Province, China, Open Forum Infect. Dis. 7 (10) (2020) ofaa430-ofaa430.
[10] Y. Shen, C. Li, H. Dong, Z. Wang, L. Martinez, Z. Sun, A. Handel, Z. Chen, E. Chen, M.H. Ebell, F. Wang, B. Yi, H. Wang, X. Wang, A. Wang, B. Chen, Y. Qi, L. Liang, Y. Li, F. Ling, J. Chen, G. Xu, Community outbreak investigation of SARS-CoV-2 transmission among bus riders in Eastern China, JAMA Intern. Med. (2020).
[11] S.M. Kissler, N. Kishore, M. Prabhu, D. Goffman, Y. Beilin, R. Landau, C. Gyamfi-Bannerman, B.T. Bateman, J. Snyder, A.S. Razavi, D. Katz, J. Gal, A. Bianco, J. Stone, D. Larremore, C.O. Buckee, Y.H. Grad, Reductions in commuting mobility correlate with geographic differences in SARS-CoV-2 prevalence in New York City, Nat. Commun. 11 (1) (2020) 4674.
[12] M. Hu, J. Wang, H. Lin, C.W. Ruktanonchai, C. Xu, B. Meng, X. Zhang, A. Carioli, Y. Feng, Q. Yin, J.R. Floyd, N.W. Ruktanonchai, Z. Li, W. Yang, A.J. Tatem, S. Lai, Risk of SARS-CoV-2 transmission among air passengers in China, Clinical infectious diseases, Off. Pub. Infectious Diseases Soc. Am. (2021).

[13] J. Rocklov, H. Sjodin, A. Wilder-Smith, COVID-19 outbreak on the Diamond Princess cruise ship: estimating the epidemic potential and effectiveness of public health countermeasures, J. Trav. Med. 27 (3) (2020) 7.
[14] A. Bak, M.A. Mugglestone, N.V. Ratnaraja, J.A. Wilson, L. Rivett, S.M. Stoneham, J. Bostock, S.E. Moses, J.R. Price, M. Weinbren, H.P. Loveday, J. Islam, A.P. R. Wilson, SARS-CoV-2 routes of transmission and recommendations for preventing acquisition: joint British infection association (BIA), healthcare infection society (HIS), infection prevention society (IPS) and Royal College of pathologists (RCPath) guidance, J. Hosp. Infect. 114 (2021) 79–103.
[15] C.V. Chapin, The Sources and Modes of Infection, Wentworth Press, 1910.
[16] S. Asadi, N. Bouvier, A.S. Wexler, W.D. Ristenpart, The coronavirus pandemic and aerosols: does COVID-19 transmit via expiratory particles? Aerosol. Sci. Technol. 54 (6) (2020) 635–638.
[17] L. Morawska, J.J. Cao, Airborne transmission of SARS-CoV-2: the world should face the reality, Environ. Int. 139 (2020) 3.
[18] P. Cheng, K. Luo, S. Xiao, H. Yang, J. Hang, C. Ou, B.J. Cowling, H.-L. Yen, D.S. C. Hui, S. Hu, Y. Li, Predominant airborne transmission and insignificant fomite transmission of SARS-CoV-2 in a two-bus COVID-19 outbreak originating from the same pre-symptomatic index case, J. Hazard Mater. 425 (2022).
[19] C. Ou, S. Hu, K. Luo, H. Yang, J. Hang, P. Cheng, Z. Hai, S. Xiao, H. Qian, S. Xiao, X. Jing, Z. Xie, H. Ling, L. Liu, L. Gao, Q. Deng, B.J. Cowling, Y. Li, Insufficient ventilation led to a probable long-range airborne transmission of SARS-CoV-2 on two buses, Build. Environ. 207 (2022).
[20] J.P. Duguid, The size and the duration of air-carriage of respiratory droplets and droplet-nuclei, J. Hyg. 44 (6) (1946) 471–479.
[21] X. Xie, Y. Li, H. Sun, L. Liu, Exhaled droplets due to talking and coughing, J. R. Soc. Interface 6 (suppl_6) (2009) S703–S714.
[22] J.K. Gupta, C.-H. Lin, Q. Chen, Transport of expiratory droplets in an aircraft cabin, Indoor Air 21 (1) (2011) 3–11.
[23] S. Zhu, J. Srebric, J.D. Spengler, P. Demokritou, An advanced numerical model for the assessment of airborne transmission of influenza in bus microenvironments, Build. Environ. 47 (2012) 67–75.
[24] C.K. Ho, R. Binns, Modeling and mitigating airborne pathogen risk factors in school buses, Int. Commun. Heat Mass Tran. 129 (2021).
[25] R.G. Loudon, R.M. Roberts, Droplet expulsion from the respiratory tract, Am. Rev. Respir. Dis. 95 (3) (1967) 435–442.
[26] S. Asadi, A.S. Wexler, C.D. Cappa, S. Barreda, N.M. Bouvier, W.D. Ristenpart, Aerosol emission and superemission during human speech increase with voice loudness, Sci. Rep. 9 (1) (2019) 2348.
[27] W.G. Lindsley, W.P. King, R.E. Thewlis, J.S. Reynolds, K. Panday, G. Cao, J. V. Szalajda, Dispersion and exposure to a cough-generated aerosol in a simulated medical examination room, J. Occup. Environ. Hyg. 9 (12) (2012) 681–690.
[28] G.R. Johnson, L. Morawska, Z.D. Ristovski, M. Hargreaves, K. Mengersen, C.Y. H. Chao, M.P. Wan, Y. Li, X. Xie, D. Katoshevski, S. Corbett, Modality of human expired aerosol size distributions, J. Aerosol Sci. 42 (12) (2011) 839–851.
[29] C.Y.H. Chao, M.P. Wan, L. Morawska, G.R. Johnson, Z.D. Ristovski, M. Hargreaves, K. Mengersen, S. Corbett, Y. Li, X. Xie, D. Katoshevski, Characterization of expiration air jets and droplet size distributions immediately at the mouth opening, J. Aerosol Sci. 40 (2) (2009) 122–133.
[30] Z.Y. Han, W.G. Weng, Q.Y. Huang, Characterizations of particle size distribution of the droplets exhaled by sneeze, J. R. Soc. Interface 10 (88) (2013) 20130560.
[31] D.A. Edwards, J.C. Man, P. Brand, J.P. Katstra, K. Sommerer, H.A. Stone, E. Nardell, G. Scheuch, Inhaling to mitigate exhaled bioaerosols, Proc. Natl. Acad. Sci. U.S.A. 101 (50) (2004) 17383–17388.
[32] A.-C. Almstrand, B. Bake, E. Ljungström, P. Larsson, A. Bredberg, E. Mirgorodskaya, A.-C. Olin, Effect of airway opening on production of exhaled particles, J. Appl. Physiol. 108 (3) (2010) 584–588.
[33] H. Holmgren, E. Ljungström, A.-C. Almstrand, B. Bake, A.-C. Olin, Size distribution of exhaled particles in the range from 0.01 to 2.0μm, J. Aerosol Sci. 41 (5) (2010) 439–446.
[34] R.G. Loudon, R.M. Roberts, Singing and the dissemination of tuberculosis, Am. Rev. Respir. Dis. 98 (2) (1968) 297–300.
[35] L. Morawska, G.R. Johnson, Z.D. Ristovski, M. Hargreaves, K. Mengersen, S. Corbett, C.Y.H. Chao, Y. Li, D. Katoshevski, Size distribution and sites of origin of droplets expelled from the human respiratory tract during expiratory activities, J. Aerosol Sci. 40 (3) (2009) 256–269.
[36] J. Lee, D. Yoo, S. Ryu, S. Ham, K. Lee, M. Yeo, K. Min, C. Yoon, Quantity, size distribution, and characteristics of cough-generated aerosol produced by patients with an upper respiratory tract infection, Aerosol Air Qual. Res. 19 (4) (2019) 840–853.
[37] L. Bourouiba, Turbulent gas clouds and respiratory pathogen emissions: potential implications for reducing transmission of COVID-19, JAMA 323 (18) (2020) 1837–1838.
[38] C.Y.H. Chao, M.P. Wan, A study of the dispersion of expiratory aerosols in unidirectional downward and ceiling-return type airflows using a multiphase approach, Indoor Air 16 (4) (2006) 296–312.
[39] C. Yang, X. Yang, B. Zhao, Person to person droplets transmission characteristics in unidirectional ventilated protective isolation room: the impact of initial droplet size, Build. Simulat. 9 (5) (2016) 597–606.
[40] S.W. Zhu, S. Kato, J.H. Yang, Study on transport characteristics of saliva droplets produced by coughing in a calm indoor environment, Build. Environ. 41 (12) (2006) 1691–1702.
[41] S.-B. Kwon, J. Park, J. Jang, Y. Cho, D.-S. Park, C. Kim, G.-N. Bae, A. Jang, Study on the initial velocity distribution of exhaled air from coughing and speaking, Chemosphere 87 (11) (2012) 1260–1264.
[42] C. Xu, P.V. Nielsen, L. Liu, R.L. Jensen, G. Gong, Human exhalation characterization with the aid of schlieren imaging technique, Build. Environ. 112 (2017) 190–199.
[43] I. Olmedo, P.V. Nielsen, M. Ruiz de Adana, R.L. Jensen, P. Grzelecki, Distribution of exhaled contaminants and personal exposure in a room using three different air distribution strategies, Indoor Air 22 (1) (2012) 64–76.
[44] J.H. Seinfeld, S.N. Pandis, Atmospheric Chemistry and Physics, from Air Pollution to Climate Change, second ed., John Wiley & Sons, Inc., New Jersey, USA, 2006.
[45] W.C. Hinds, Aerosol Technology: Properties, Behavior, and Measurement of Airborne Particles, second ed., Wiely, New York, USA, 1999.
[46] R.M. Effros, K.W. Hoagland, M. Bosbous, D. Castillo, B. Foss, M. Dunning, M. Gare, W. Lin, F. Sun, Dilution of respiratory solutes in exhaled condensates, Am. J. Respir. Crit. Care Med. 165 (5) (2002) 663–669.
[47] M. Nicas, W.W. Nazaroff, A. Hubbard, Toward understanding the risk of secondary airborne infection: emission of respirable pathogens, J. Occup. Environ. Hyg. 2 (3) (2005) 143–154.
[48] W. Chen, N. Zhang, J. Wei, H.-L. Yen, Y. Li, Short-range airborne route dominates exposure of respiratory infection during close contact, Build. Environ. 176 (2020), 106859.
[49] X.Y. Li, B. Liu, S.Z. Li, S.S. Liu, Numerical simulations of biological droplet transport in an indoor environment, Adv. Mater. Res. 356–360 (2012) 862–866.
[50] B. Wang, A. Zhang, J.L. Sun, H. Liu, J. Hu, L.X. Xu, Study of SARS transmission via liquid droplets in air, J. Biomech. Eng. 127 (1) (2005) 32–38.
[51] X. Xie, Y. Li, A.T.Y. Chwang, P.L. Ho, W.H. Seto, How far droplets can move in indoor environments – revisiting the Wells evaporation–falling curve, Indoor Air 17 (3) (2007) 211–225.
[52] C.Y.H. Chao, M.P. Wan, G.N. Sze To, Transport and removal of expiratory droplets in hospital ward environment, Aerosol. Sci. Technol. 42 (5) (2008) 377–394.
[53] B. Zhao, Z. Zhang, X. Li, Numerical study of the transport of droplets or particles generated by respiratory system indoors, Build. Environ. 40 (8) (2005) 1032–1039.
[54] K. Talaat, M. Abuhegazy, O.A. Mahfoze, O. Anderoglu, S.V. Poroseva, Simulation of aerosol transmission on a Boeing 737 airplane with intervention measures for COVID-19 mitigation, Phys. Fluids 33 (3) (2021), 033312.
[55] F. Yao, X. Liu, The effect of opening window position on aerosol transmission in an enclosed bus under windless environment, Phys. Fluids 33 (12) (2021).
[56] X. Yang, C. Ou, H. Yang, L. Liu, T. Song, M. Kang, H. Lin, J. Hang, Transmission of pathogen-laden expiratory droplets in a coach bus, J. Hazard Mater. 397 (2020).
[57] W. Duan, D. Mei, J. Li, Z. Liu, M. Jia, S. Hou, Spatial distribution of exhalation droplets in the bus in different seasons, Aerosol Air Qual. Res. 21 (8) (2021).
[58] C.C. Ooi, A. Suwardi, Z.L.O. Yang, G. Xu, C.K.I. Tan, D. Daniel, H.Y. Li, Z.W. Ge, F. Y. Leong, K. Marimuthu, O.T. Ng, S.B. Lim, P. Lim, W.S. Mak, W.C.D. Cheong, X. J. Loh, C.W. Kang, K.H. Lim, Risk assessment of airborne COVID-19 exposure in social settings, Phys. Fluids 33 (8) (2021).
[59] L. Yang, M. Li, X. Li, J. Tu, The effects of diffuser type on thermal flow and contaminant transport in high-speed train (HST) cabins - a numerical study, Int. J. Vent. 17 (1) (2018) 48–62.
[60] L. Zhang, Y. Li, Dispersion of coughed droplets in a fully-occupied high-speed rail cabin, Build. Environ. 47 (2012) 58–66.
[61] S. Ko, S.-B. Kwon, W. Jeong, D. Park, Numerical analysis of droplets exhaled by train cabin passengers, J. Odor Indoor Environ. 18 (2) (2019) 131–139.
[62] H.A. Elmaghraby, Y.W. Chiang, A.A. Aliabadi, Ventilation strategies and air quality management in passenger aircraft cabins: a review of experimental approaches and numerical simulations, Sci. Technol. Built Environ. 24 (2) (2018) 160–175.
[63] M. Mesgarpour, J.M.N. Abad, R. Alizadeh, S. Wongwises, M.H. Doranehgard, S. Ghaderi, N. Karimi, Prediction of the spread of Corona-virus carrying droplets in a bus-A computational based artificial intelligence approach, J. Hazard Mater. 413 (2021).
[64] T. Moreno, R. Maria Pinto, A. Bosch, N. Moreno, A. Alastuey, M. Cruz Minguillon, E. Anfruns-Estrada, S. Guix, C. Fuentes, G. Buonanno, L. Stabile, L. Morawska, X. Querol, Tracing surface and airborne SARS-CoV-2 RNA inside public buses and subway trains, Environ. Int. 147 (2021).
[65] M. Hadei, S.R. Mohebbi, P.K. Hopke, A. Shahsavani, S. Bazzazpour, M. Alipour, A. J. Jafari, A.M. Bandpey, A. Zali, M. Yarahmadi, M. Farhadi, M. Rahmatinia, V. Hasanzadeh, S.S.H. Nazari, H. Asadzadeh-Aghdaei, M. Tanhaei, M.R. Zali, M. Kermani, M.H. Vaziri, H. Chobineh, Presence of SARS-CoV-2 in the air of public places and transportation, Atmos. Pollut. Res. 12 (3) (2021) 255–259.
[66] G. Caggiano, F. Apollonio, F. Triggiano, G. Diella, P. Stefanizzi, M. Lopuzzo, M. D'Ambrosio, N. Bartolomeo, G. Barbuti, G.T. Sorrenti, P. Magarelli, D. P. Sorrenti, V. Marcotrigiano, O. De Giglio, M.T. Montagna, SARS-CoV-2 and public transport in Italy, Int. J. Environ. Res. Publ. Health 18 (21) (2021).
[67] P. Di Carlo, P. Chiacchiaretta, B. Sinjari, E. Aruffo, L. Stuppia, V. De Laurenzi, P. Di Tomo, L. Pelusi, F. Potenza, A. Veronese, J. Vecchiet, K. Falasca, C. Ucciferri, Air and surface measurements of SARS-CoV-2 inside a bus during normal operation, PLoS One 15 (11) (2020) e0235943-e0235943.
[68] Y. Tsuchihashi, T. Yamagishi, M. Suzuki, T. Sekizuka, M. Kuroda, T. Itoi, A. Matsumura, N. Yamada, Y. Ishii, N. Kawamura, Y. Hitomi, T. Hiroshima, K. Azuma, K. Saito, N. Kawanishi, S. Tanaka, R. Yamaguchi, K. Yano, T. Sunagawa, High attack rate of SARS-CoV-2 infections during a bus tour in Japan, J. Trav. Med. 28 (8) (2021).
[69] V. Vlacha, G. Feketea, A. Petropoulou, S.D. Tranca, The significance of duration of exposure and circulation of fresh air in SARS-CoV-2 transmission among healthcare workers, Front. Med. 8 (2021).

[70] D.W.E. Ramirez, M.D. Klinkhammer, L.C. Rowland, COVID-19 transmission during transportation of 1st to 12th grade students: experience of an independent school in Virginia, J. Sch. Health 91 (9) (2021) 678–682.
[71] L. Steinwender, D. Holy, J. Burkhard, I. Uckay, Daily use of public transportation and incidence of symptomatic COVID-19 among healthcare workers during the peak of a pandemic wave in Zurich, Switzerland, Am. J. Infect. Control (2021).
[72] L. Bandiera, G. Pavar, G. Pisetta, S. Otomo, E. Mangano, J.R. Seckl, P. Digard, E. Molinari, F. Menolascina, I.M. Viola, Face coverings and respiratory tract droplet dispersion, R. Soc. Open Sci. 7 (12) (2020) 201663.
[73] D. Carrion, E. Colicino, N.F. Pedretti, K.B. Arfer, J. Rush, N. DeFelice, A.C. Just, Neighborhood-level disparities and subway utilization during the COVID-19 pandemic in New York City, Nat. Commun. 12 (1) (2021).
[74] S. Fathi-Kazerooni, R. Rojas-Cessa, Z. Dong, V. Umpaichitra, Correlation of subway turnstile entries and COVID-19 incidence and deaths in New York City, Infectious Disease Modelling 6 (2021) 183–194.
[75] K.T.L. Sy, M.E. Martinez, B. Rader, L.F. White, Socioeconomic Disparities in Subway Use and COVID-19 Outcomes in New York City, medRxiv : the Preprint Server for Health Sciences, 2020.
[76] S. Hamidi, I. Hamidi, Subway ridership, crowding, or population density: determinants of COVID-19 infection rates in New York city, Am. J. Prev. Med. 60 (5) (2021) 614–620.
[77] S.H. Bae, H. Shin, H.-Y. Koo, S.W. Lee, J.M. Yang, D.K. Yon, Asymptomatic transmission of SARS-CoV-2 on evacuation flight, Emerg. Infectious Disease J. 26 (11) (2020) 2705.
[78] P.B. Blomquist, H. Bolt, S. Packer, U. Schaefer, S. Platt, G. Dabrera, M. Gobin, I. Oliver, Risk of symptomatic COVID-19 due to aircraft transmission: a retrospective cohort study of contact-traced flights during England's containment phase, Influenza Other Respir, Viruses 15 (3) (2021) 336–344.
[79] E. Choi, D.K.W. Chu, P.K.C. Cheng, D.N.C. Tsang, M. Peiris, D. Bausch, L.L. M. Poon, D. Watson-Jones, In-flight transmission of SARS-CoV-2, Emerg. Infectious Disease J. 26 (11) (2020) 2713.
[80] N.C. Khanh, P.Q. Thai, H.L. Quach, N.A.H. Thi, P.C. Dinh, T.N. Duong, L.Q. T. Mai, N.D. Nghia, T.A. Tu, L.N. Quang, T.D. Quang, T.T. Nguyen, F. Vogt, D. D. Anh, Transmission of SARS-CoV-2 during long-haul flight, Emerg. Infect. Dis. 26 (11) (2020) 2617–2624.
[81] R. Nir-Paz, I. Grotto, I. Strolov, A. Salmon, M. Mandelboim, E. Mendelson, G. Regev-Yochay, Absence of in-flight transmission of SARS-CoV-2 likely due to use of face masks on board, J. Trav. Med. 27 (8) (2020).
[82] K.L. Schwartz, M. Murti, M. Finkelstein, J.A. Leis, A. Fitzgerald-Husek, L. Bourns, H. Meghani, A. Saunders, V. Allen, B. Yaffe, Lack of COVID-19 transmission on an international flight, Can. Med. Assoc. J. 192 (15) (2020). E410-E410.
[83] P. Okada, R. Buathong, S. Phuygun, T. Thanadachakul, S. Parnmen, W. Wongboot, S. Waicharoen, S. Wacharapluesadee, S. Uttayamakul, A. Vachlraphan, M. Chittaganpitch, N. Mekha, N. Janejai, S. Iamsirithaworn, R.T. C. Lee, S. Maurer-Stroh, Early transmission patterns of coronavirus disease 2019 (COVID-19) in travellers from Wuhan to Thailand, Euro Surveill. 25 (8) (2020) 6–10. January 2020.
[84] J.K. Pang, S.P. Jones, L.L. Waite, N.A. Olson, J.W. Armstrong, R.J. Atmur, J. J. Cummins, Probability and estimated risk of SARS-CoV-2 transmission in the air travel system, Trav. Med. Infect. Dis. 43 (2021).
[85] J.J. Zhang, F. Qin, X.Y. Qin, J.R. Li, S.J. Tian, J. Lou, X.Q. Kang, H.X. Lian, S. M. Niu, W.Z. Zhang, Y.G. Chen, Transmission of SARS-CoV-2 during air travel: a descriptive and modelling study, Ann. Med. 53 (1) (2021) 1569–1575.
[86] H. Speake, A. Phillips, T. Chong, C. Sikazwe, A. Levy, J. Lang, B. Scalley, D. Speers, D. Smith, P. Effler, S. McEvoy, Flight-associated transmission of severe acute respiratory syndrome coronavirus 2 corroborated by whole-genome sequencing, Emerg. Infectious Disease J. 26 (12) (2020) 2872.
[87] T. Toyokawa, T. Shimada, T. Hayamizu, T. Sekizuka, Y. Zukeyama, M. Yasuda, Y. Nakamura, S. Okano, J. Kudaka, T. Kakita, M. Kuroda, T. Nakasone, Transmission of SARS-CoV-2 during a 2-h domestic flight to Okinawa, Japan, Influenza and Other Respiratory Viruses 16 (1) (2022) 63–71. March 2020.
[88] J. Chen, H. He, W. Cheng, Y. Liu, Z. Sun, C. Chai, Q. Kong, W. Sun, J. Zhang, S. Guo, X. Shi, J. Wang, E. Chen, Z. Chen, Potential transmission of SARS-CoV-2 on a flight from Singapore to Hangzhou, China: an epidemiological investigation, Trav. Med. Infect. Dis. 36 (2020), 101816.
[89] S. Hoehl, O. Karaca, N. Kohmer, S. Westhaus, J. Graf, U. Goetsch, S. Ciesek, Assessment of SARS-CoV-2 transmission on an international flight and among a tourist group, JAMA Netw. Open 3 (8) (2020) e2018044-e2018044.
[90] E. Mun, Y.-M. Kim, B. Han, J. Jeong, W. Kim, C. Lee, A case series of flight attendants at risk of COVID-19 in South Korea in 2020, Ann. Occup. Environ. Med. 33 (1) (2021).
[91] A. Pavli, P. Smeti, S. Hadjianastasiou, K. Theodoridou, A. Spilioti, K. Papadima, A. Andreopoulou, K. Gkolfinopoulou, S. Sapounas, N. Spanakis, A. Tsakris, H. C. Maltezou, In-flight transmission of COVID-19 on flights to Greece: an epidemiological analysis, Trav. Med. Infect. Dis. 38 (2020) 3.
[92] K. Hayakawa, S. Kutsuna, T. Kawamata, Y. Sugiki, C. Nonaka, K. Tanaka, M. Shoji, M. Nagai, S. Tezuka, K. Shinya, H. Saito, T. Harada, N. Moriya, M. Tsuboi, M. Norizuki, Y. Sugiura, Y. Osanai, M. Sugiyama, A. Okuhama, K. Kanda, Y. Wakimoto, M. Ujiie, S. Morioka, K. Yamamoto, N. Kinoshita, M. Ishikane, S. Saito, Y. Moriyama, M. Ota, K. Nakamura, T. Nakamoto, S. Ide, H. Nomoto, Y. Akiyama, T. Suzuki, Y. Miyazato, Y. Gu, N. Matsunaga, S. Tsuzuki, Y. Fujitomo, Y. Kusama, H. Shichino, M. Kaneshige, J. Yamanaka, M. Saito, M. Hojo, M. Hashimoto, S. Izumi, J. Takasaki, M. Suzuki, K. Sakamoto, Y. Hiroi, S. Emoto, M. Tokuhara, T. Kobayashi, K. Tomiyama, F. Nakamura, N. Ohmagari, H. Sugiyama, SARS-CoV-2 infection among returnees on charter flights to Japan from Hubei, China: a report from National Center for Global Health and Medicine, Glob. Health Med. 2 (2) (2020) 107–111.
[93] T. Lytras, G. Dellis, A. Flountzi, S. Hatzianastasiou, G. Nikolopoulou, K. Tsekou, Z. Diamantis, G. Stathopoulou, M. Togka, G. Gerolymatos, G. Rigakos, S. Sapounas, S. Tsiodras, High prevalence of SARS-CoV-2 infection in repatriation flights to Greece from three European countries, J. Trav. Med. 27 (3) (2020).
[94] H.A. Thompson, N. Imai, A. Dighe, K.E.C. Ainslie, M. Baguelin, S. Bhatia, S. Bhatt, A. Boonyasiri, O. Boyd, N.F. Brazeau, L. Cattarino, L.V. Cooper, H. Coupland, Z. Cucunuba, G. Cuomo-Dannenburg, B. Djaafara, I. Dorigatti, S. van Elsland, R. FitzJohn, H. Fu, K.A.M. Gaythorpe, W. Green, T. Hallett, A. Hamlet, D. Haw, S. Hayes, W. Hinsley, B. Jeffrey, E. Knock, D.J. Laydon, J. Lees, T.D. Mangal, T. Mellan, S. Mishra, A. Mousa, G. Nedjati-Gilani, P. Nouvellet, L. Okell, K. V. Parag, M. Ragonnet-Cronin, S. Riley, H.J.T. Unwin, R. Verity, M. Vollmer, E. Volz, P.G.T. Walker, C. Walters, H. Wang, Y. Wang, O.J. Watson, C. Whittaker, L.K. Whittles, P. Winskill, X. Xi, C.A. Donnelly, N.M. Ferguson, SARS-CoV-2 infection prevalence on repatriation flights from Wuhan City, China, J. Trav. Med. 27 (8) (2020).
[95] O.T. Ng, K. Marimuthu, P.Y. Chia, V. Koh, C.J. Chiew, L.D. Wang, B.E. Young, M. Chan, S. Vasoo, L.M. Ling, D.C. Lye, K.Q. Kam, K.C. Thoon, SARS-CoV-2 infection among travelers returning from Wuhan, China, N. Engl. J. Med. 382 (15) (2020) 1476–1478.
[96] H. Lei, Y. Li, S. Xiao, C.H. Lin, S.L. Norris, D. Wei, Z. Hu, S. Ji, Routes of transmission of influenza A H1N1, SARS CoV, and norovirus in air cabin: comparative analyses, Indoor Air 28 (3) (2018) 394–403.
[97] H. Lei, Y.G. Li, S.L. Xiao, X.Y. Yang, C.H. Lin, S.L. Norris, D. Wei, Z.M. Hu, S.C. Ji, Logistic growth of a surface contamination network and its role in disease spread, Sci. Rep. 7 (2017) 10.
[98] L.M. Casanova, S. Jeon, W.A. Rutala, D.J. Weber, M.D. Sobsey, Effects of air temperature and relative humidity on coronavirus survival on surfaces, Appl. Environ. Microbiol. 76 (9) (2010) 2712–2717.
[99] A.J. Prussin, D.O. Schwake, K. Lin, D.L. Gallagher, L. Buttling, L.C. Marr, Survival of the enveloped virus Phi6 in droplets as a function of relative humidity, absolute humidity, and temperature, Appl. Environ. Microbiol. 84 (12) (2018) e00551-18.
[100] K. Lin, L.C. Marr, Humidity-dependent decay of viruses, but not bacteria, in aerosols and droplets follows disinfection kinetics, Environ. Sci. Technol. 54 (2) (2020) 1024–1032.
[101] W. Yang, S. Elankumaran, L.C. Marr, Relationship between humidity and influenza A viability in droplets and implications for influenza's seasonality, PLoS One 7 (10) (2012), e46789.
[102] Y. Feng, T. Marchal, T. Sperry, H. Yi, Influence of wind and relative humidity on the social distancing effectiveness to prevent COVID-19 airborne transmission: a numerical study, J. Aerosol Sci. 147 (2020), 105585.
[103] A. Ahlawat, A. Wiedensohler, S.K. Mishra, An overview on the role of relative humidity in airborne transmission of SARS-CoV-2 in indoor environments, Aerosol Air Qual. Res. 20 (9) (2020) 1856–1861.
[104] H. Dai, B. Zhao, Association of the infection probability of COVID-19 with ventilation rates in confined spaces, Build. Simulat. 13 (6) (2020) 1321–1327.
[105] H. Furuya, Risk of transmission of airborne infection during train commute based on mathematical model, Environ. Health Prev. Med. 12 (2) (2007) 78–83.
[106] W.C. Hill, M.S. Hull, R.I. MacCuspie, Testing of commercial masks and respirators and cotton mask insert materials using SARS-CoV-2 virion-sized particulates: comparison of ideal aerosol filtration efficiency versus fitted filtration efficiency, Nano Lett. 20 (10) (2020) 7642–7647.
[107] E. O'Kelly, S. Pirog, J. Ward, P.J. Clarkson, Ability of fabric face mask materials to filter ultrafine particles at coughing velocity, BMJ Open 10 (9) (2020), e039424.
[108] C.D. Zangmeister, J.G. Radney, E.P. Vicenzi, J.L. Weaver, Filtration efficiencies of nanoscale aerosol by cloth mask materials used to slow the spread of SARS-CoV-2, ACS Nano 14 (7) (2020) 9188–9200.
[109] M. Zhao, L. Liao, W. Xiao, X. Yu, H. Wang, Q. Wang, Y.L. Lin, F.S. Kilinc-Balci, A. Price, L. Chu, M.C. Chu, S. Chu, Y. Cui, Household materials selection for homemade cloth face coverings and their filtration efficiency enhancement with triboelectric charging, Nano Lett. 20 (7) (2020) 5544–5552.
[110] M.A. Boraey, An analytical model for the effective filtration efficiency of single and multiple face masks considering leakage, Chaos, Solitons & Fractals 152 (2021), 111466.
[111] A.C.K. Lai, C.K.M. Poon, A.C.T. Cheung, Effectiveness of Facemasks to Reduce Exposure Hazards for Airborne Infections Among General Populations, 9, 2012, pp. 938–948, 70.
[112] S. Asadi, C.D. Cappa, S. Barreda, A.S. Wexler, N.M. Bouvier, W.D. Ristenpart, Efficacy of masks and face coverings in controlling outward aerosol particle emission from expiratory activities, Sci. Rep. 10 (1) (2020) 15665.
[113] N.H.L. Leung, D.K.W. Chu, E.Y.C. Shiu, K.-H. Chan, J.J. McDevitt, B.J.P. Hau, H.-L. Yen, Y. Li, D.K.M. Ip, J.S.M. Peiris, W.-H. Seto, G.M. Leung, D.K. Milton, B. J. Cowling, Respiratory virus shedding in exhaled breath and efficacy of face masks, Nat. Med. 26 (5) (2020) 676–680.
[114] A.H. Heald, M. Stedman, Z. Tian, P. Wu, A.A. Fryer, Modelling the impact of the mandatory use of face coverings on public transport and in retail outlets in the UK on COVID-19-related infections, hospital admissions and mortality, Int. J. Clin. Pract. 75 (3) (2021), e13768.
[115] D.O. Freedman, A. Wilder-Smith, In-flight transmission of SARS-CoV-2: a review of the attack rates and available data on the efficacy of face masks, J. Trav. Med. 27 (8) (2020).
[116] Y. Cheng, N. Ma, C. Witt, S. Rapp, P.S. Wild, M.O. Andreae, U. Poschl, H. Su, Face Masks Effectively Limit the Probability of SARS-CoV-2 Transmission, Science, New York, N.Y., 2021.